AN ABSTRACT OF THE THESIS OF

George Hunt Kennedy (Name) for the Ph. D. (Degree) in Chemistry (Major)

Date thesis is presented _____

Title SORPTION BY DETACHED ORGANIC FILMS AND ITS RELATION TO FILIFORM CORROSION

Abstract approved [redacted] (Major Professor)

The rate of interaction of carbon dioxide with eight detached organic films commonly used as coatings for metal surfaces was examined. The films studied were lacquers of several different formulations including oleoresinous, phenolic, vinyl, alkyd, epoxy, and hydrocarbon types. The sorption was measured on a McBain type gravimetric adsorption balance fitted with quartz helixes with an extension sensitivity of about one mm./mg. Rates of sorption were measured at three temperatures, -45.3° C., -63.5° C. and -76.5° C., and at three pressures at each temperature, 461.0 torr, 326.5 torr and 117.5 torr. Theoretical examination of the data lead to the conclusion that the rate controlling mechanism was a diffusion process. Sorption coefficients were calculated from the kinetic data and limiting diffusion coefficients determined by extrapolation to zero $CO_2$ activity. Values on the order of $10^{-12}$ $cm.^2/sec.$ were obtained. From these were calculated activation energies for the diffusion process, which were compared to the calculated isosteric heats of sorption.

Oxygen sorption isotherms were attempted and no oxygen uptake was detected. A few water vapor rate experiments were performed for comparison with the $CO_2$ results. The rate of water vapor interaction was found to be two to three orders of magnitude faster than that for $CO_2$.

The eight films studied have been rated as to their relative resistance to filiform corrosion growth. This relative resistance to filiform corrosion was compared with the relative diffusion rate of $CO_2$. A correlation is suggested, with the films showing faster $CO_2$ uptake also showing the most resistance. This is in agreement with the observed effect that $CO_2$ in a corrosion test atmosphere inhibits filiform corrosion growth.

# SORPTION BY DETACHED ORGANIC FILMS AND ITS RELATION TO FILIFORM CORROSION

by

GEORGE HUNT KENNEDY

A THESIS

submitted to

OREGON STATE UNIVERSITY

in partial fulfillment of
the requirements for the
degree of

DOCTOR OF PHILOSOPHY

June 1966

APPROVED: [redacted]

Professor of Chemistry
In Charge of Major

[redacted]

Chairman of Department of Chemistry

[redacted]

Dean of Graduate School

Date thesis is presented Sept. 1, 1965

Typed by Marcia Ten Eyck

## ACKNOWLEDGEMENT

I would like to express my gratitude to Dr. W. H. Slabaugh for his encouragement throughout the course of this investigation and for his help in the interpretation of the results. Appreciation is extended to the Paint Research Institute, whose financial aid in part made this study possible. Thanks is also given to Dr. R. R. Ryan for his help in programing the Elovich calculations.

Special thanks is extended to my wife, Kay, for her moral support, tangible aid, and constant encouragement, without which I might never have written this thesis.

TABLE OF CONTENTS

LIST OF FIGURES

LIST OF TABLES

# SORPTION BY DETACHED ORGANIC FILMS AND ITS RELATION TO FILIFORM CORROSION

## INTRODUCTION

A phenomenon known as filiform corrosion has offered a unique opportunity to apply a basic research approach to a problem generally attacked with technological tools. It has become apparent that protective coatings play an important part in the mechanism of this paradoxical form of corrosion. Thus it was anticipated that a basic research investigation of the surface properties of a series of corrosion inhibiting coatings might reveal new knowledge of the filiform process. The work presented here consists mainly of an investigation of the rate of interaction of carbon dioxide with eight polymer coatings under which filiform corrosion grows with varying degrees of ease. Some information on oxygen and water interaction with these coatings is also presented.

### History of Filiform Corrosion

Man has long been concerned with the deteriorating effect of corrosion and recent technology has made tremendous advances in its control, but one form of corrosion has proved to be an anomaly. It generally exists only when the metal has been protected from other forms of corrosion by some type of protective coating. This strange corrosion behavior was first noted in the literature by Sharman (25)

and it was he who termed it "filiform". It has since become a well identified form of corrosion, occurring in thread-like filaments spread out on the metal surface immediately beneath the coating. When active, the filaments consist of a "head" and a "tail". On steel the tail is made up of a solid, reddish colored corrosion product while the head consists of a bluish fluid. This liquid head, round in front with a V-shaped edge sharply separating it from the dry red deposit of rust behind, is the active part of the filament, progressing along the metal surface and depositing behind it the solid corrosion product. A normal filiform filament can be from 0. 1 to 0. 5 millimeters wide and several hundred times as long. It can progress at the rate of about 0. 5 millimeters per day and will generally travel in a straight line until it collides with a previously deposited filament, whereby it will alter course. Figures 1 and 2 show typical filiform growth on steel.

Rather specific conditions are required for filiform activity (34). It occurs on steel at room temperature only between 65 and 95 percent relative humidity, wider filaments being observed at the higher water vapor concentrations. It has also been observed on aluminum, magnesium and a variety of other metals. Several mechanisms have been proposed to explain its growth, but a clear picture of the phenomenon has been hampered by the complexity of the problem. Apparently the corrosion grows as the result of the interplay between the

FIGURE I. FILIFORM GROWTH ON A STEEL PANEL WITH ALKYD COATING, ACTUAL SIZE. PANEL EXPOSED TO 80 PERCENT RELATIVE HUMIDITY.

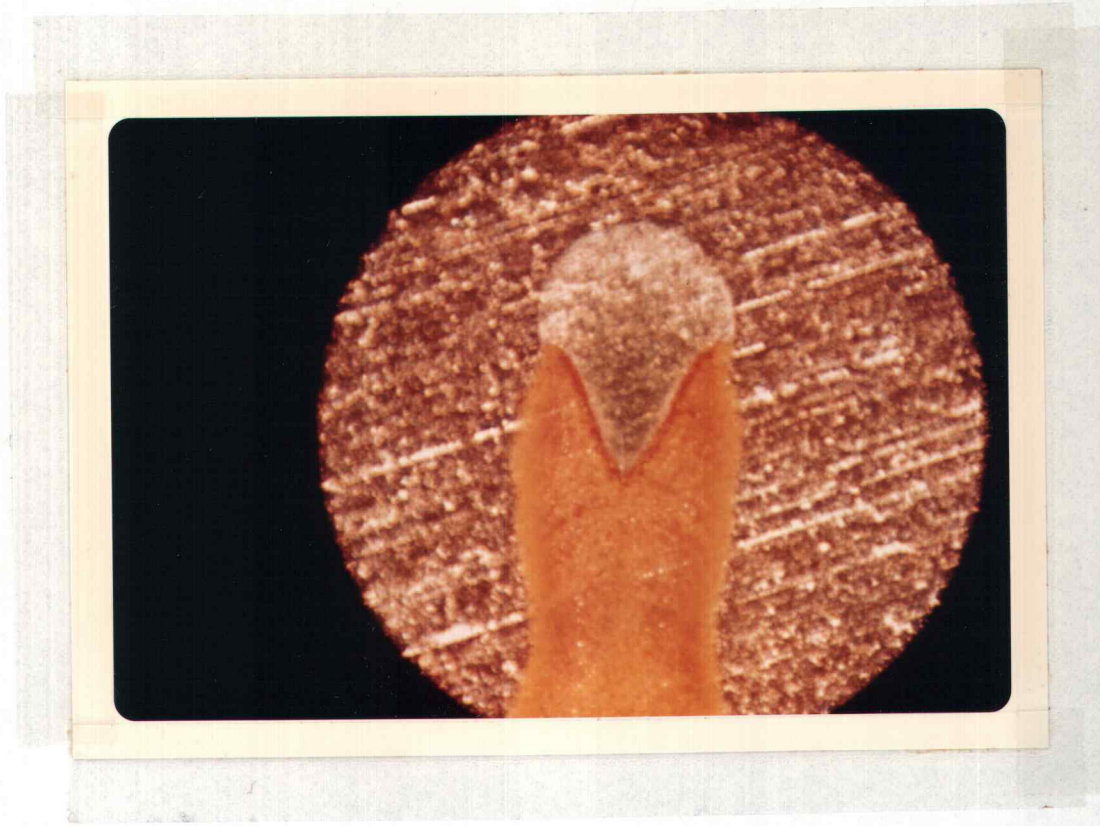

FIGURE 2. PHOTOMICROGRAPH OF ACTIVE HEAD OF FILIFORM FILAMENT ON STEEL WITH VINYL COATING, 50X. PANEL EXPOSED TO 80 PERCENT RELATIVE HUMIDITY.

atmosphere, its water vapor activity, a surface film on the metal, and the metal surface itself. Even though filiform has been reported on supposedly bare metals, it is assumed that some type of film is actually present, such as an oxide film on the surface of aluminum.

Van Loo and coworkers (34) attempted to explain filiform by a mechanism involving an initiating force, a driving force, and a directing force. They suggested that corrosion anodes are initiated by an electrolytic mechanism as in ordinary corrosion. The driving force is the diffusion of the corrosive atmosphere into the active head, resulting in further metallic corrosion. The directing force is explained on the basis of concentration cells. Slabaugh and Grotheer (27) investigated the electro-chemical properties of filiform, actually measuring the electro-potential between anodic and cathodic areas. They developed a theory based on the osmotic transfer of solvent water through a semipermeable organic coating.

Preston and Sanyal (23) and Kaesche (12) have emphasized the role of the relative humidity in filiform corrosion, basing their investigations on artificial seeding of the metal-coating system with salt nuclei. According to Preston and Sanyal, the corrosion is initiated by the adsorption of water vapor on the surfaces of the salt nuclei, forming a saturated solution which then corrodes electrolytically. Kaesche classified various nuclei as to their relative effectiveness for initiating filiform. Some correlation exists between the

relative humidity over saturated solutions of the various salts and their effectiveness in initiating corrosion. Those salts whose saturated solutions exhibit relative humidities in the range previously determined to be optimum for filiform growth (34) are most effective. According to Kaesche, the steady growth of filiform, both with respect to width and rate of linear movement, is attributed to the preservation of a critical amount of electrolyte carried along by the head from the point of origin.

## Practical Significance and Control

Filiform corrosion is not structurally significant because of its slight depth of penetration into the metal, on the order of 0.005 millimeters. However it does drastically disfigure a metal surface and can contribute to the deterioration of paint films and the initiation of other forms of corrosion. It was initially of major concern in the can lining industry where it was easily observed because most can linings are clear varnishes or lacquers. It can occur with relatively high speed. Thus a large surface may be subjected to extensive filiform growth within a period of months. The full extent of its occurrence is not known, owing to the fact that it occurs frequently under opaque coatings where its detection is difficult.

There is no satisfactory method of controlling filiform corrosion. Certain steps can be taken however. By controlling the relative

humidity below 50 or 60 percent the corrosion can be prevented. As indicated, the protective film plays an important role in the corrosion mechanism. If some coating is used, such as a paraffin film, which is highly impermeable to water, filiform can be avoided. Correspondingly, a completely permeable membrane, such as a paint formulated with a pigment volume above the critical pigment volume concentration (CPVC) (1) will also prevent filiform growth. The CPVC is the maximum concentration of pigment at which film continuity can still exist. If the film is not continuous, it will be completely permeable. However, exceeding the CPVC detracts from other protective qualities of the film.

## Organic Films

Most theories proposed to explain filiform corrosion support the view that the protective film plays a leading role in the process. Hence it would seem that the characteristics of the film used to protect metal from corrosion hold a valuable key to the full understanding of the corrosion mechanism. With this in mind, Slabaugh, et al. (26) initiated a study of a series of various types of films commonly used for corrosion protection. Emphasis has been placed on investigating the sorption of atmospheric gases on these films as these are no doubt also involved in the corrosion process. The present work is an extension of this study.

Eight films were used in this series of investigations and are listed in Table I along with some of their physical properties. The films were prepared as coatings on steel and tin plate carefully selected from production stock commonly used for making cans. Coatings were applied by means of a roller application at controlled thickness and baked at 180° C. except for the vinyl films, which were baked at 150° C.

Table I. Specifications of films examined.

| Sample Number | Type | Applied Weight, mg./cm.$^2$ | Free Film Thickness x $10^4$ cm. | Filiform Corrosion Performance*(8) |
|---|---|---|---|---|
| 1 | Oleoresinous | 0.85 | 7.9 | 6 |
| 2 | Phenolic | 0.66 | 8.9 | 8 |
| 3 | Vinyl (Heavy) | 1.01 | 10.2 | 1 |
| 4 | Vinyl (Light) | 0.50 | 5.6 | 2 |
| 5 | Alkyd | 0.85 | 7.9 | 3 |
| 6 | Epoxy | 0.66 | 7.1 | 4 |
| 7 | Hydrocarbon A | 0.70 | 8.6 | 5 |
| 8 | Hydrocarbon B | 0.78 | 8.9 | 7 |

* Higher number indicates better ability to prevent filiform corrosion.

The oleoresinous film is a common type of varnish which is a combination of oils, resins, thinner and driers.

Phenolic resins are obtained by reacting fomaldehyde or other aldehydes with phenol or a substituted phenol. They form surface coatings without the necessity of using oil by the reaction between chains to produce crosslinking. The basic reaction may be written,

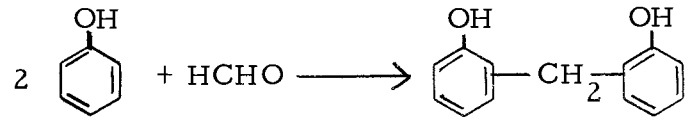

The vinyl film used in this study is a solution coating of a copolymer of vinyl chloride and vinyl acetate. The basic reaction involved in its synthesis is,

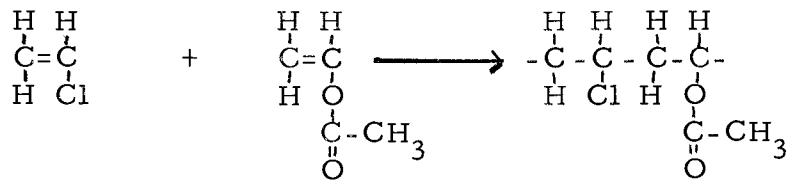

The vinyl polymers polymerize linearly, normally exhibiting no cross-linking.

Alkyd or polyester films are formed from a polyhydric alcohol such as glycerol and a polybasic acid or its anhydride such as phthalic anhydride. Often fatty acid side chains are present which have the effect of limiting molecular weight. The principal reaction involved is esterification,

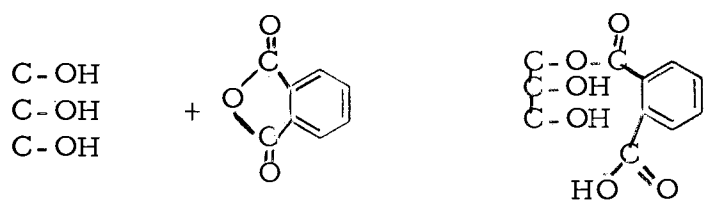

Epoxy resins are formed by condensation, in the presence of alkali, of epichlorhydrin with a dihydric phenol,

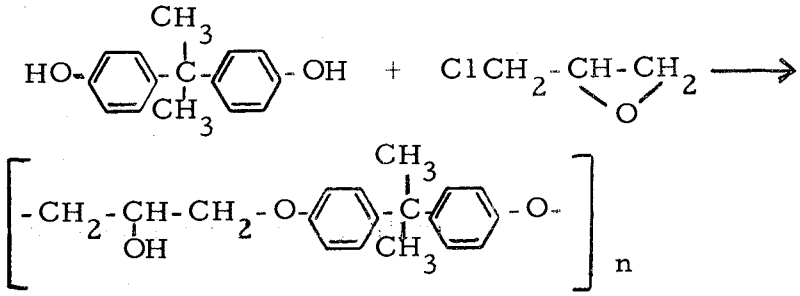

High temperatures induce cross-linking in this polymer.

The basic polymerization reaction entering into the production of typical aliphatic hydrocarbon films is represented by,

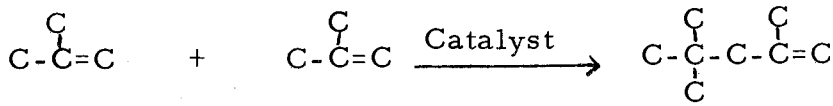

They are essentially non-conjugated diolefins. The difference between Hydrocarbon A and Hydrocarbon B listed in Table I is that the polymerization of B was catalyzed with phosphoric acid. Both underwent peroxide catalysis.

Slabaugh, et al. (26) studied the water vapor sorption by the eight organic films. They obtained adsorption isotherms at three different temperatures from which was determined the number of active sites for water vapor adsorption and the parameters in the classical Brunauer, Emmett and Teller (BET) (3) isotherm equation. They detected differences in the films caused by the method of removal from the metal substrate and concluded that those removed by

amalgamation with mercury were most similar in total structure to the original films. They also observed a rate effect in the water sorption but only qualitative information was obtained.

The investigation of water vapor interaction was extended by Slabaugh and Kennedy (28), who obtained equilibrium adsorption-desorption isotherms from which were calculated pore size distributions. These calculations rested upon the assumption that the hysteresis effect they observed was caused by capillary condensation and the lowering of vapor pressure over a concave meniscus. They attempted to correlate the calculated pore radii with filiform corrosion performance and found at least some qualitative correlation.

Patterson (20) looked at nitrogen and carbon dioxide sorption by the films and made some tentative conclusions about the type of interaction occurring. No uptake of nitrogen was observed but carbon dioxide sorption with a pronounced rate effect was noted. The interaction was interpreted in terms of the empirical Elovich rate law of chemisorption (17), although only a limited amount of data were available.

The work presented in this thesis includes oxygen sorption, an extensive study of the rate of interaction of carbon dioxide, and a few quantitative measurements of the rate of water vapor sorption by the eight organic films noted above.

# THEORETICAL BACKGROUND

## Adsorption

Adsorption can be defined generally as that phenomenon which results in a concentration or accumulation of substances at surfaces or interfaces. This may involve two rather distinct types of interaction. The first, called chemisorption, is due to the primary valence forces of the interacting substances and is largely independent of the physical character of the adsorbent. It is a chemical reaction and generally involves a large evolution of heat. The second more general type is called physical adsorption and arises from physical forces between adsorbent and adsorbate of the van der Waals type. Physical adsorption can be considered as an act of condensation of a gas upon the surface of a solid and involves a rather low evolution of heat, in the range of the heat of liquefaction. In some cases a clear cut division between the two types of adsorption is not possible. Young and Crowell (35, p. 1-3) have listed the following criteria for distinguishing between them.

(a) The heat of physical adsorption is of the same order of magnitude as the heat of liquefaction of the adsorbate, whereas the heat of chemisorption is of the same order of magnitude as that of the corresponding bulk chemical reaction. In some cases, however, very low heats of chemisorption are found.

(b) Physical adsorption, like condensation, is a general phenomenon and will occur with any gas-solid system provided only that the conditions of temperature and pressure are suitable. On the other hand, chemisorption will occur only if the gas is capable of forming a chemical bond with the surface atoms.

(c) A physically adsorbed gas may be removed by reducing the pressure, at the temperature at which adsorption took place, although the process may be slow on account of diffusion effects. The removal of a chemisorbed gas, however, often requires much more severe conditions; higher temperatures are generally required.

(d) Under suitable conditions of temperature and pressure, physically adsorbed layers several molecules thick are frequently found. In contrast, chemisorption is usually complete once a monomolecular layer is built up, although physical adsorption may occur on top of chemisorption.

(e) Since physical adsorption is related to the process of condensation, it occurs to an appreciable extent at pressures and temperatures close to those required for liquefaction. There are some exceptions, notably with adsorbents having very fine pores. On the other hand, chemisorption often proceeds at much lower pressures and much higher temperatures.

(f) Physical adsorption and chemisorption may sometimes be distinguished by the different rates of approach to equilibrium.

Physical adsorption per se is instantaneous but, with some adsorbents, diffusion of the gas into the adsorbent mass is often slow, particularly at low pressures. Chemisorption may be instantaneous but there are many systems where chemisorption involves an activation energy. The use of rate criterion to distinguish physical from chemical adsorption is thus filled with uncertainties. Mathematical analysis of the rates involved, however, often helps to clarify the situation.

Taken together these different criteria are usually sufficient to enable one to decide between physical adsorption and chemisorption. The occasional borderline cases reflect the fact that in essence all forces of adsorption are electrical in origin so that the division of adsorption phenomena into physical and chemical is, in the ultimate, merely one of convenience.

## Theories of Adsorption

Ever since the observations of Scheele in 1773 on the adsorption of gases by charcoal, there have been attempts to derive a theoretical basis for the phenomena. One of the oldest attempted explanations is the empirical expression of Freundlich, who related the amount of gas adsorbed with pressure. The equation is as follows:

$$x/m = K P^{1/n} \qquad [1]$$

where x/m is the weight of adsorbate per gram of adsorbent, P is the pressure, and K and n are constants.

In 1915 Langmuir (15) proposed one of the first and most important equations based on theory. He envisioned adsorption as a type of chemical combination or process in which the adsorbed layer was unimolecular. He obtained experimental verification of his theory from a series of determinations on the adsorption of gases at low pressures on plane surfaces such as mica and glass. The Langmuir isotherm takes the following form:

$$P/V = 1/V_m b + P/V_m \qquad [2]$$

where V is the volume of gas adsorbed at pressure P, $V_m$ is the volume adsorbed when the surface is covered with a complete monolayer, and b is a constant for any specific temperature.

The Langmuir theory is limited by the fact that it considers only a monolayer and that it predicts a saturation value for the amount of adsorption. However, for those same reasons it has been used successfully to explain many cases of chemisorption.

When experimental evidence for adsorption in layers more than one molecule thick began to mount, attempts were made to modify Langmuir's equation to fit multi-layer adsorption. Brunauer, Emmett and Teller (3) in 1938 derived an isotherm equation for multimolecular layers from data obtained from low temperature gas

adsorption on an iron synthetic ammonia catalyst. It is very similar to Langmuir's equation for unimolecular layers, and its use was soon adopted for a very wide range of adsorbents and adsorbates. The major assumption in the BET theory is that the same forces that produce condensation are also responsible for multimolecular adsorption. The derivation of the BET equation results in the following expression for the formation of a monolayer:

$$P/V(P_o-P) = (1/V_mC) - \left[(C-1)/V_mC\right] \ (P/P_o) \qquad [3]$$

where P is the measured pressure, $P_o$ is the saturation pressure, V is the volume adsorbed at pressure P, $V_m$ is the volume adsorbed on a monolayer, and C is a constant related to the heat of adsorption.

If a plot of $P/V(P_o-P)$ versus $P/P_o$ is made from experimentally obtained values, a straight line is obtained for values of $P/P_o$ from 0.05 to 0.35 for a system that conforms to the BET theory. It can now be seen from the above equation that the slope of this line is $(C-1)/V_mC$ and the intercept on the ordinate is $1/V_mC$. Two equations can be set up with two unknowns and solved for $V_m$ which gives:

$$V_m = 1/(\text{intercept} + \text{slope}) \qquad [4]$$

With a value for $V_m$ the surface area covered by a monolayer can be readily calculated provided the effective cross-sectional area of the adsorbed molecule is known. The area used is usually found from the known density of the liquified or solidified adsorbate and to the

extent that this value is valid, the BET theory provides an absolute method for determining the surface area of a solid.

Since the above theory was proposed, many theoretical adsorption isotherms have appeared in the literature. However, the BET theory is still the most widely accepted method for explaining experimental adsorption data and calculating surface areas.

## Thermodynamics of Adsorption

The adsorption of gases by a solid is always accompanied by an evolution of heat. This evolution is usually determined by two different methods. The first method is direct calorimetric measurement as the adsorption takes place. A volume of gas is admitted to the surface of the solid and the heat evolved is calculated from the temperature increase. This is an average heat for a specific part of the surface covered and is known as the integral heat of adsorption, $Q_i$. To be thermodynamically correct, as the integral heat of adsorption is normally defined, it should be measured in a system where no PV work is occurring. This is the case in a sorption system where the adsorbate is allowed to expand into an evacuated chamber containing the adsorbent.

The heat evolved when an infinitesimal amount of gas is adsorbed is known as the differential heat of adsorption, $Q_d$, and can be measured approximately by adding minute quantities of gas at a time to

the surface. This quantity is the one normally measured in calorimetric studies of adsorption.

A second method of arriving at heats of adsorption involves the relationship between the temperature variation of the adsorbate pressure, at constant surface coverage, and the heat of adsorption. The relationship is simply a specialized application of the Clausius-Clapeyron equation and the heat derived is called the isosteric heat, $Q_{st}$:

$$(\partial \ln P/\partial T)_{\Theta} = Q_{st}/RT^2 \qquad [5]$$

where $\Theta$ is the degree of surface coverage.

The isosteric heat at any value $\Theta$ can be calculated graphically from the above equation by plotting the adsorption isostere as ln P versus 1/T and determining the slope, which equals $-Q_{st}/R$. This method does not require the assumption that $Q_{st}$ is constant with T but isotherm measurements are required at three temperatures, preferably even more. More commonly, the integrated form of the above equation is used:

$$\ln(P_2/P_1) = Q_{st}(T_2 - T_1)/R(T_2T_1) \qquad [6]$$

or

$$Q_{st} = 2.303R \left[T_2T_1/(T_2 - T_1)\right] \left[\log(P_2/P_1)\right] \qquad [7]$$

where only isotherms at two temperatures are needed.

It is possible to show by the use of thermodynamics that $Q_{st} = Q_d + RT$. In actual calorimetric measurements, the differential heat determined would probably lie somewhere between $Q_{st}$ and $Q_d$, since usually there is some exchange of work between portions of the gas and not all of the gas would lie within the calorimeter. However, the difference, RT, is normally smaller than the error of measurements. The isosteric or differential heat of adsorption is generally plotted against the amount of surface coverage, $\Theta$. The magnitude of the heat normally decreases with coverage, a phenomenon usually attributed to surface heterogeneity in which sites of lessening energy are covered as adsorption proceeds. In some cases, adsorption heats are seen to rise with coverage. This is usually explained on the basis of surface homogeneity with lateral adsorbate interaction.

## Hysteresis

With regard to thermodynamic calculations, one troublesome point must be mentioned. These calculations of course presuppose the existence of reversibility. Contrary to this assumption, many adsorbent-adsorbate systems exhibit hysteresis; that is, the adsorption and desorption branches of the isotherm do not match. This phenomenon precludes the existence of reversibility and throws doubt on any thermodynamic calculations made for such a system. Although calculations on such systems will have no absolute significance, they

are still used widely for comparative purposes between series of samples all showing similar behavior (6).

No explanation has yet been proposed for hysteresis that fits all experimental data, and it is probably correct to say that hysteresis can be caused by several different factors, one or all of which may be applicable to a specific system. The explanation generally attributed for it is capillary condensation. The capillaries fill by multilayer adsorption, but once filled they desorb by evaporation from a meniscus. The lowering of the vapor pressure associated with a meniscus of a very small radius is the cause of the hysteresis loop. Pierce and Smith (21) however, have pointed out that hysteresis can be caused by condensation and evaporation effects without the presence of capillaries. They claim that hysteresis is found when adsorption occurs by merging clumps or islands of molecules on separate sites of a plane surface. After the islands merge, all molecules are held by forces from all active sites touched by the merged group. Forces are therefore stronger than when the groups were separate, the vapor pressures of all molecules are lowered and there is desorption hysteresis.

The second widely accepted theory to explain hysteresis postulates structural changes within the framework of the adsorbent. This could involve some type of rearrangement of a crystal lattice due to interaction with the adsorbate, change in particle size or aggregation,

and swelling effects. Hirst (9) attempted to construct models to explain the various forms of hysteresis. He states that swelling may bring about a distortion of the adsorbent in such a manner as to cause the adsorbent structure to spring open at a certain point and thus open up areas previously closed, leading to a sudden increase in adsorption. This could be followed by a new stage where the swelling would again be limited by elastic restraint until the surface pressure again causes the structure to open up. On desorption this sequence of events would occur in reverse. However, since surface forces fall off rapidly with distance, they are weaker when the structure is open than those which originally resisted the opening. Therefore, on returning to the surface pressure which caused the structure to spring open, there is no sudden collapse; the structure remains open until the surface pressure falls sufficiently to be overcome by the diminished surface forces. Thus there is hysteresis.

## Chemisorption Kinetics

As stated earlier, physical adsorption is essentially instantaneous unless other factors such as diffusion are operative. Chemisorption, on the other hand, often shows a rate effect indicating an activation energy. Many cases of chemisorption of gases on solids proceeding at a measureable rate can be found in the literature. Numerous attempts to represent the experimental data by algebraic

mass-action functions or by the partial pressure of gas and a constant rate parameter of definite order have not been successful (17). Similarly, various empirical expressions for chemisorption kinetics were often unconvincing and limited to the particular adsorbate-absorbent system under consideration. One empirical expression, however, has been shown to be generally applicable to chemisorption kinetics (30). This is the Elovich equation, most often seen in the differential form:

$$dq/dt = \underline{a} \exp(-\alpha q) \qquad [8]$$

where q is the amount adsorbed at time t, and $\underline{a}$ and $\alpha$ are constant during any one experiment. It is seen that the rate decreases exponentially with the amount of gas adsorbed.

Calculation of rate parameters by direct application of Equation 8 involves a graphical differentiation or a calculation ofrates averaged over short time intervals. These procedures are difficult and generally lend themselves to large errors. Thus the Elovich equation is generally applied in its integrated form.

Assuming that $q = 0$ at $t = 0$, the equation becomes

$$q = (1/\alpha) \ln(1 + a\alpha t) \qquad [9]$$

or

$$q = (1/\alpha) \ln (t + t_o) - (1/\alpha) \ln t_o \qquad [10]$$

with

$$t_o = 1/\underline{a}\alpha \qquad [11]$$

Equation 10 has the form of a straight line and when q is plotted as a function of $\ln(t+t_o)$, it provides a test of the Elovich equation. The rate parameter, $\alpha$, is found from the slope, and $\underline{a}$ from Equation 11. The parameter $t_o$ is found by trial and error. With a correctly chosen $t_o$, the plot gives a straight line; with $t_o$ too small, the plot is convex, and with $t_o$ too large, it is concave to the axis of $\ln(t+t_o)$. This method also may yield imprecise and misleading results, mainly due to the difficulty of choosing a unique value of $t_o$; often a rather wide range of values gives a reasonably linear plot of q versus $\ln(t+t_o)$.

A more precise method for testing the Elovich equation has been described by Sarmousakis and Low (24) and is the method used in this investigation. For comparison, checks were made with the method of plotting q versus $\ln(t+t_o)$. Starting from Equation 8 and integrating from some initial conditions $(t_1, q_1)$ to running conditions (t, q), it is possible to put the Elovich equation into a very workable form. Proceeding from the differential form of the Elovich equation

$$dq/dt = \underline{a} \exp(-\alpha q) \qquad [8]$$

and rearranging to

$$(1/\underline{a}) \exp(\alpha q)\, dq = dt \qquad [12]$$

integration between t and $t_1$, and q and $q_1$ gives

$$1/\underline{a}\,[\{\exp(\alpha q)/\alpha\} - \{\exp(\alpha q_1)/\alpha\}] = t - t_1 \qquad [13]$$

or

$$\exp(\alpha q) - \exp(\alpha q_1) = \underline{a}\alpha t - \underline{a}\alpha t_1 \qquad [14]$$

which can be rearranged to give

$$\exp(\alpha q) - \underline{a}\alpha t = \exp(\alpha q_1) - \underline{a}\alpha t_1 = \text{a constant, C.} \qquad [15]$$

The running conditions ($q_1$, $t_1$) were not restricted or limited and thus Equation 15 holds for any position on the sorption curve. In other words it is constant for any specific system if the original expression, the Elovich equation, actually describes the system. A test of fit of Equation 8 and concurrent evaluation of $\underline{a}$ and $\alpha$ may be carried out using experimental values of $q_{mt}$, $q_{nt}$ and $q_{pt}$ determined at times mt, nt and pt, respectively; m, n and p being integers. Solving Equation 15 for q:

$$q = (1/\alpha)\,[\ln \underline{a}\alpha + \ln\{t + (C/\underline{a}\alpha)\}] \qquad [16]$$

and taking the experimental values at times mt, nt and pt,

$$q_{nt} - q_{mt} = (1/\alpha)\,\ln\frac{1 + ny}{1 + my} \qquad [17]$$

or

$$\frac{q_{nt} - q_{mt}}{q_{pt} - q_{mt}} = \frac{\ln\frac{1 + ny}{1 + my}}{\ln\frac{1 + py}{1 + my}} = D(y) \qquad [18]$$

where $y = \underline{a}\alpha t/C$. A table of D as a function of y for appropriate values of m, n and p permits evaluation of y from the experimental value of D, if Equation 8 applies. Substitution of y in Equation 17 gives $\alpha$, and substitution of $\alpha$ and $t/y = c/\underline{a}$ in Equation 16 yields the correct value of $\underline{a}$. Agreement with each other of the estimates of $\underline{a}$ and $\alpha$ for successively increasing values of mt serves as a sensitive indication of fit of the Elovich equation.

A completely adequate theory to explain Elovich kinetics has not yet been proposed. Especially difficult to resolve are the abrupt inflections often found in Elovich plots [q versus $\ln(t+t_o)$] and the significance of changes in $\underline{a}$ and $\alpha$ as the temperature or pressure is changed. Taylor and Thon's (30) interpretation is the most widely accepted. The mechanism proposed by them is as follows:

a) Surface sites active to the chemisorbable gas do not pre-exist, but a quasi-explosive production of sites results upon contact with the gas. This results in an initial steady-state site concentration marked by a more or less considerable massive amount adsorbed, $q_{t_o}$.

b) Following step a), production of new sites having ceased definitely, slow adsorption sets in, with bimolecular disappearance of sites and correspondingly exponential decline of the rate of adsorption. The decay of sites involves site-site interaction and repeated site-molecule collisions resulting in annihilation of a number of sites

prior to adsorption of the molecule. The rate is pressure independent, governed solely by the availability of sites.

When q, the amount adsorbed, equals zero, it is seen from Equation 8 that $\underline{a}$ represents the initial rate of adsorption. The mass action of the gas governs this initial rate so $\underline{a}$ is proportional to the gas pressure and increases with rising temperature. It is found that $\underline{a}$ derived from treatment of the data by the Elovich equation is much smaller than the experimentally observed value, $\underline{a}_{ob.}$, which is obtained from the initial slope of the rate of adsorption. This supports Taylor and Thon's view of a very rapid massive initial adsorption not governed by the exponential law.

Further examination of Equation 8 leads to some insight as to the physical significance of $\alpha$. To be compatible with Elovich kinetics, the number of sites, n must be given by

$$n = n_o \exp(-\alpha q) \qquad [19]$$

where $n_o$ is the number of sites at $q = 0$. The corresponding differential form is

$$-\frac{dn}{dq} = \alpha n \qquad [20]$$

which expresses the fact that the decrease of n with increasing q is proportional to n. The rate of site incapacitation is

$$-\frac{dn}{dt} = \alpha n \frac{dq}{dt} \qquad [21]$$

which demonstrates that $\alpha$ represents the rate of site decay for a given site concentration and rate of adsorption. The value of $\alpha$ corresponds to the efficiency of site annihilation by an interacting gas molecule; it expresses the probability of the annihilation of sites upon repeated site-molecule interaction, leading to the mechanism proposed by Taylor and Thon. A plain molecule-per-site inactivation would call for $-dn/dq$ = constant, which, referring to Equation 20 is seen to be inconsistant with Elovich kinetics.

Experimentally, $\alpha$ normally decreases slightly with increasing initial pressure. A sudden change of pressure in later stages of adsorption, however, usually causes no change in $\alpha$, demonstrating its independency of pressure, reflecting the sole dependency of the slow adsorption rate on the concentration of sites. With rising temperature, $\alpha$ decreases or increases depending on the gas-solid system and the temperature range studied.

The effects of temperature on chemical reactions are generally described in terms of the Arrhenius equation:

$$d \ln k/dT = E_a/RT^2 \qquad [22]$$

where k is the specific rate constant, R is the gas constant, and $E_a$ is the energy of activation. Applying the equation to chemisorption controlled by Elovich kinetics is beset with complications, mainly due to the impossibility of calculating specific rate constants.

Modified versions of the Arrhenius equation have been used, substituting terms such as $\ln v_2/v_1$ or $\ln t_1/t_2$ for $\ln k$, where $v_2/v_1$ is the ratio of velocities at the two temperatures taken at the same quantity adsorbed, or where $t_1/t_2$ is the ratio of times required for the adsorption of a given amount. Much evidence indicates that the adsorption processes at each temperature are occurring on different areas and thus have no connection with one another. Thus the above terms cannot properly be used in the Arrhenius equation. The activation energies can only be derived in those cases where the given amount of gas is adsorbed on the same area at the two different temperatures. Other substitutions have been made but they all suffer from the drawback mentioned above. In view of the uncertainty of choice of comparable stages of adsorption, the significance of $E_a$ must be reduced from an energy of activation to a mere temperature coefficient. This lead Low (17) to state that if knowledge of such a temperature coefficient is desirable, simpler and less ambiguous expressions such as

$$(\alpha_1/\alpha_2)/(T_2/T_1) \qquad [23]$$

are preferable.

## Diffusion

A second explanation for observing a rate effect in sorption is that the sorption is diffusion controlled. Diffusion is defined as that

process by which matter is transported from one part of a system to another by random molecular, atomic or ionic motion. It was first put on a quantitative basis by Fick who derived two basic equations by recognizing the relationship between diffusion and the transfer of heat by conduction (5, p. 1-3). Fick's first equation is based on the hypothesis that the rate of transfer of a diffusing substance through a unit area of a section is proportional to the concentration gradient measured normal to the section. That is:

$$P = -D\, dc/dx \qquad [24]$$

where P is the rate of permeation per unit area in the steady state of flow, c is the concentration of diffusing substance, x is the space coordinate measured normal to the section, and D is called the diffusion coefficient. In some cases, for example diffusion in dilute solutions, D can reasonably be taken as constant while in others, such as some cases of diffusion in high polymers, it depends strongly on concentration. If P, the amount of material diffusing, and c, the concentration, are both expressed in terms of the same unit of quantity, then it is clear that D is independent of this unit and has dimensions of length$^{2}$ time$^{-1}$. The negative sign in Equation 24 arises because diffusion occurs in the opposite direction from that of increasing concentration.

Derived from Equation 24 is Fick's second law for non-steady

state permeation (5, p. 3-5), which takes the form:

$$\frac{dc}{dt} = D \frac{d^2c}{dx^2} \qquad [25]$$

where t is the time and D, c and x are defined the same as in Equation 24. General solutions of the diffusion equations have been obtained for a variety of initial and boundary conditions when the diffusion coefficient is constant. The solutions are usually either comprised of a series of error functions or take the form of a converging trigonometric series.

Of specific interest in diffusion studies is the determination of D and its concentration dependence from experimental data. Two basic experimental methods are used when investigating diffusion through membranes or films. First is the permeation method, a steady-state procedure in which the rate of penetrant transferred through a membrane is determined. The system under study is mounted between two sections of a chamber. The system is evacuated and the gas is admitted at a specific pressure to one side of the cell. As it permeates the film the pressure increase in the second chamber is recorded as a function of time. Solutions to Fick's laws have been derived to fit the boundary conditions present in this type of experiment which allow the calculation of D.

The second technique, a sorption method, is a transient state procedure in which the mass of penetrant gained or lost by the

membrane when exposed to different, but constant, vapor activity is followed gravimetrically (22). As gas penetrates the film from both sides, the rate of weight increase and the final equilibrium value are recorded. In this experiment the boundary conditions are c equals $c_1$ at x equal to 0 and x equal to L (film thickness) for all t; c equals 0 at any point within the film at t equal to 0; further, the areas of the two faces of the membrane are so much greater than the area of the edges that the diffusion may be considered to be one-dimensional. Barrer (2, p. 7-17) solved Fick's differential equation of diffusion for the general case of sorption kinetics arriving at:

$$q = L\left[\frac{c_1 + c_2}{2} + c_o\right]\left[1 - \frac{8}{\pi^2}\sum_{m=0}^{\infty}\frac{1}{(2m+1)^2}\exp\left\{\frac{-D(2m+1)^2\pi^2 t}{L^2}\right\}\right] \quad [26]$$

where $c_1$ is the vapor concentration in the film at x equal to 0, $c_2$ is the vapor concentration in the film at x equal to L, $c_o$ is the vapor concentration in the film at t equal to 0, m equals 0, 1, 2. . . ., and q is the weight change (sorption or desorption) at time t. When, as above, $c_o$ equals 0, $c_1$ equals $c_2$, and recognizing that the product of L and $c_1$ equals $q_e$, the equilibrium weight change, Equation 26 becomes:

$$\frac{q}{q_e} = 1 - \frac{8}{\pi^2}\sum_{m=0}^{\infty}\frac{1}{(2m+1)^2}\exp\left\{\frac{-(2m+1)^2\pi^2 Dt}{L^2}\right\} \quad [27]$$

The application of Equation 26 or 27 also assumes that immediately upon placing the film in the presence of the vapor, the concentration at each surface attains a value equal to the eventual equilibrium uptake of the film as a whole. Since the series involved in Equation 27 converges rapidly, for times slightly larger than zero only the first term of the series is of consequence during most of the sorption or desorption. Considering only this first term, Long and Thompson (16) simplified this to:

$$\frac{d\,[\log\,(q_e - q)]}{dt} = \frac{-\,\pi^2 D}{2.3\,L^2} \qquad [28]$$

This gives both an experimental test for the constancy of D and a method to evaluate D when it is independent of concentration. The log of $(q_e - q)$ is plotted against time. A straight line indicates that D is constant and it can be evaluated from the slope which is equivalent to $-\pi^2 D/2.3L^2$.

Again looking at Equation 27, the value of $t/L^2$ for which $q/q_e$ equals one-half, conveniently written $(t/L^2)_{1/2}$, is approximately given by (5, p. 240-241):

$$\left(\frac{t}{L^2}\right)_{1/2} = \frac{1}{\pi^2 D}\,\ln\frac{\pi^2}{16} - \frac{1}{9}\left(\frac{\pi^2}{16}\right)^9 \qquad [29]$$

or

$$D = 0.049/(t/L^2)_{1/2} \qquad [30]$$

The error in this approximate method for determining D was given by Crank to be 0.001 percent. If D is concentration dependent, Equation 30 would give an average diffusion coefficient, $\bar{D}$. It is also possible to deduce an average diffusion coefficient from the initial slope of the reduced sorption curve, that is $q/q_e$ versus $\sqrt{t}/L$ (5, p. 247-248). Thus in the early stages, for a constant diffusion coefficient D and a sheet thickness L, Crank derived the expression:

$$\frac{q}{q_e} = \frac{4}{\pi^{1/2}} \left( \frac{Dt}{L^2} \right)^{1/2} \qquad [31]$$

If the initial slope, S, of the reduced sorption curve is observed in a sorption experiment in which D is concentration dependent, then the average diffusion coefficient, $\bar{D}$, is approximately:

$$\bar{D} = \frac{\pi}{16} S^2 \qquad [32]$$

By taking the slope when $q/q_e$ equals one-half, it is easily seen that Equations 30 and 32 are equivalent.

A more exact determination can be made of D, when it is concentration dependent, from the Boltzmann solution of Fick's law, as pointed out by Long and Thompson (16). For the initial stages of either sorption or desorption:

$$q/q_e = K \sqrt{t}/L \qquad [33]$$

If this equation is obeyed, implying Fickian diffusion, the integral diffusion coefficient for a given equilibrium concentration, c, can be obtained from the equation:

$$\bar{D}(c) = \frac{1}{c} \int_{c_o}^{c} D \, dc = \frac{\pi}{32} \left( K_s^2 (0, c) + K_d^2 (c, 0) \right) \qquad [34]$$

where $K_s$ and $K_d$ are the initial slopes of plots of $q/q_e$ versus $\sqrt{t}/L$ for sorption and desorption, respectively, between the concentrations 0 and c. It is also found that if D (or $\bar{D}$) increases with concentration, $K_s$ is greater than $K_d$; whereas if D is independent of concentration, $K_s$ equals $K_d$. In the case where $K_s$ equals $K_d$, Equation 34 becomes:

$$D = \frac{\pi}{32} K^2 \qquad [35]$$

which is seen to be the same as Equation 32 and thus will also reduce to Equation 30 at $q/q_e$ equal to one-half.

In all cases thus far the expressions derived hold only for Fickian diffusion, defined experimentally when the reduced sorption curve gives a straight line over most of its course. The following gives a summary of the features of particular importance in Fickian diffusion (7, p. 6-7):

a) Both sorption and desorption curves are linear in the region of small values of the abscissa.

b) The slope of both the sorption and desorption curves is concave against the abscissa above the linear portion.

c) The shape of the sorption curve is not very sensitive to the concentration dependence of D.

d) The sorption or desorption curves for membranes differing only in thickness with the same final penetrant concentration have identical slopes.

e) A sorption and desorption curve will coincide if D is concentration independent, the sorption will lie above the desorption curve if D is concentration dependent.

Sorption which is non-Fickian is defined as that which does not give an initially linear reduced sorption curve. Fujita (7, p. 13-14) also summarizes some of the representative anomalies found in these systems:

a) In the region of small $\sqrt{t}/L$, both the sorption and desorption curves are not linear.

b) The sorption curve has an inflection point.

c) For systems with D dependent on concentration, the paired sorption-desorption curves cross.

d) Sorption and desorption curves obtained from varying thickness experiments cannot be reduced to a single curve.

The calculation of diffusion coefficients from non-Fickian sorption curves is, because of non-linearity, necessarily ambiguous. The sorption half times are known, however, and an average sorption coefficient, $\bar{R}$, may be defined as (11)

$$\bar{R} = 0.049/(t/L^2)_{1/2} \qquad [36]$$

which is a comparative measure of the sorption rate. Of course, $\bar{R}$ equals $\bar{D}$, for reduced sorption curves which are linear through their half-times. As the vapor activity is reduced, non-Fickian reduced sorption curves generally approach linearity. Thus a limiting diffusion coefficient may be determined if sorption coefficients as a function of activity are available,

$$\lim_{a \to 0} \bar{R} = \lim_{a \to 0} \bar{D} = D_o \qquad [37]$$

where a is the activity of the vapor and $D_o$ is the limiting diffusion coefficient.

An insight into the mechanism of diffusion in polymer films is given by the transition state theory. Glasstone, Laidler, and Eyring (8, p. 516-544) discuss the application of this theory to the passage of gases through membranes. Diffusion is pictured as taking place discontinuously, depending on the random motion of the polymer segments, a void or hole being formed by their movement. If this occurs in the vicinity of the diffusant, the gas can then occupy this free space. The length the gas or vapor molecules move in going from "hole" to "hole" is called the "jump" distance, $\lambda$. The transition state is then the molecular sized void and the activation energy is considered to be that necessary to cause the polymer segments to move in such a way as to form this opening. The energy of

separation of the diffusant from its neighbors is assumed to be negligible. In accordance with the transition state theory, Glasstone, et al. gives

$$D = A \exp(-E_a/RT) \qquad [38]$$

where D is the diffusion coefficient, A is a constant related to the jump distance and the entropy change in a diffusion step, and $E_a$ is the activation energy, R and T being the gas constant and temperature, respectively. They further show that

$$A = e\lambda^2 \frac{kT}{h} \exp(S^{\ddagger}/R) \qquad [39]$$

where $\lambda$ is as defined above, e is the base of natural logarithms, h is Plank's constant and $S^{\ddagger}$ the entropy change associated with a unit diffusion step. It is now possible to calculate A and $E_a$ from experimental determinations of the diffusion coefficient at two or more temperatures and, by means of Equation 39 to calculate $\lambda^2 \exp(S^{\ddagger}/R)$ or its square root. This value will give some indication of the entropy of activation for the diffusion process.

In connection with explaining non-Fickian diffusion using transition state theory arguments, a commonly referred to property of polymers must be introduced. This is the glass transition temperature, $T_g$. All polymers undergo a sudden transition at some specific temperature that manifests itself in many ways, such as viscosity changes, volume-temperature discontinuities, a sudden specific

heat jump, and so on, all occurring at the specific temperature, $T_g$. This transition is attributed to a quasi-phase change where the polymer suddenly becomes more rigid or glassy. Above $T_g$, the polymer segments are less constrained and are free to oscillate and rotate. Below $T_g$, segmental motion is believed to be minimal. It is the movement of these segments which provide the openings by which the gas transport process through polymers takes place. Above $T_g$ Fickian sorption is normally observed. Below $T_g$ many systems show non-Fickian sorption properties. Any structural feature which affects the interchain attraction or mobility will be important in determining the diffusion rates. Thus anomalous diffusion behavior below $T_g$ would be expected.

# EXPERIMENTAL METHODS AND APPARATUS

## Description of Apparatus

The sorption data were determined gravimetrically on an adsorption balance of a type first described by McBain and Bakr (18). It is shown diagramatically in Figure 3. Two reservoirs, one for liquid storage and one for gas storage, were located on the main manifold for easy addition of adsorbate. An adsorbate fractionation train was attached and used when necessary. The manifold was fitted with the standard pressure measuring devices; a mercury manometer, an oil manometer filled with Dow Corning 703 fluid, and a McLeod gauge. A second manifold was connected to the main manifold, and eight adsorption columns were connected to it, each fitted with an individual stopcock so they could be isolated from the system.

The springs used for the balance were small, quartz helixes, each with a sensitivity of about one millimeter extension per milligram. The samples were suspended from the springs via fine glass fiber extension rods which contained coded colored markings for measurement purposes. The bulk of the adsorption columns, containing the springs, was enclosed in a constant temperature air bath maintained at $35.0 \pm 0.2^{\circ}$ C. This was found to be sufficient to prevent any spring response changes. The lower portion of the adsorption columns enclosing the samples was kept at constant temperature

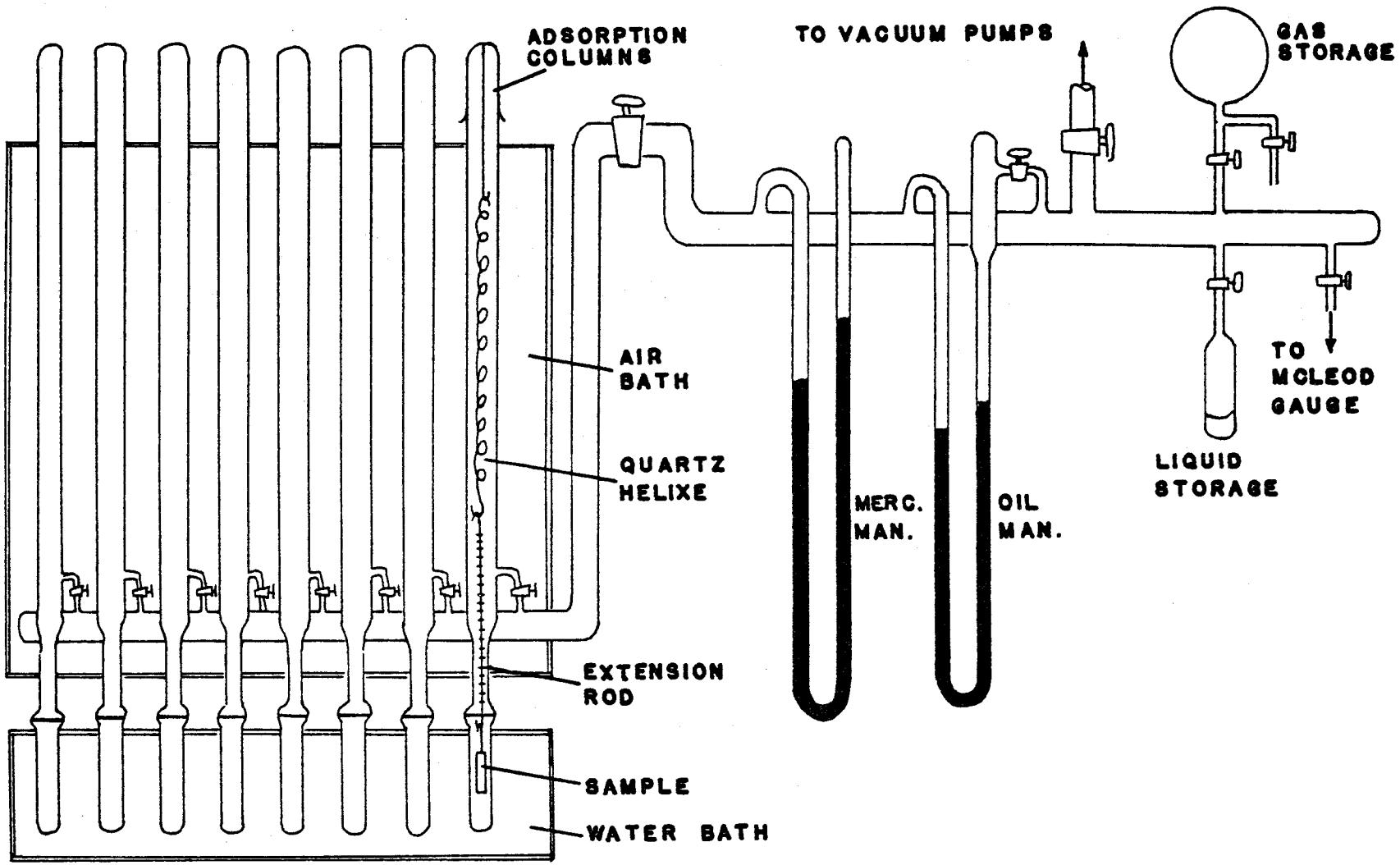


FIGURE 3. GRAVIMETRIC ADSORPTION BALANCE

using a water bath for runs near room temperature, a dry ice-isopropyl alcohol bath, slush baths, or liquid nitrogen. The spring extensions were magnified by optically projecting the colored markings of the extension rods upon a wall chart about 15 feet in front of the sample tubes. The extensions were read in scale divisions of the wall chart. Each spring was calibrated by adding known weights, and a spring constant was calculated in milligrams per scale division. The sensitivity of the extension readings was about 0.2 milligrams per division and the scale could be read to 0.1 divisions for an overall sensitivity of $\pm$ 0.02 milligrams for a 300 milligram sample.

## Preparation of Samples

The eight organic polymer films used were freshly removed from tin plate. As indicated previously, the work of Slabaugh, et al. (26) indicated some structural differences between films removed by the amalgamation process and by an electrolysis process. In the latter the metal plate is made the cathode in a one percent sodium carbonate solution. Platinum gauze serves as an anode. The films come off at a potential of 12 volts, requiring only seconds for the vinyls but up to several hours for the epoxy and hydrocarbon films. Slabaugh, et al. concluded that this more vigorous treatment altered the structure of the films more severely than the former process. Hence this work was done on films removed by the mercury

amalgamation technique.

The edges of the coated panels were placed in a shallow pool of mercury. In a few minutes, the resulting tin amalgam at the film-metal interface destroyed the adhesion of the films and they were readily lifted from the panel. They were then flushed carefully with distilled water to remove any clinging droplets of mercury and dried at room temperature. The dried films were stored in closed jars at room conditions until used.

To prepare the films for investigation, several strips about eight by twenty centimeters were loosely rolled and weighed on an analytical balance. Samples of about 250-350 milligrams were prepared. The rolls were then tied with fine copper-beryllium wire and suspended from the quartz helixes by means of a glass fiber hooked at the bottom end. The fiber passed through the center of the roll of film, hooking around the bottom lip of the roll. The samples were then outgassed for 24 hours at room temperature and $10^{-3}$ torr, the loss in weight being subtracted from that previously determined. Thus the sample weights used in all calculations are those of the outgassed sample in vacuum, that is with no buoying effect. Before each sorption experiment the samples were outgassed at $10^{-3}$ torr for 48 hours at room temperature. This was seen to be sufficient as the original sample weights were always achieved by outgassing them following a sorption run.

## Experimental Procedure

### Carbon Dioxide Sorption

The source of carbon dioxide used was freshly crushed dry ice. This was cooled to liquid nitrogen temperature and evaculated at $10^{-3}$ torr for three to four hours. The temperature was then raised with a dry ice-isopropyl alcohol bath and the $CO_2$ gas was allowed to expand through two more dry ice-isopropanol cold traps into a third trap at liquid nitrogen temperature where it was collected. After collecting, it was isolated from the previous traps and again outgassed at $10^{-3}$ torr for one-half hour. The liquid nitrogen was then replaced by dry ice-isopropanol once more and as the $CO_2$ pressure increased the gas was allowed to expand into the gas storage bulb for subsequent use.

Carbon dioxide sorption was investigated extensively at three different pressures, each pressure studied at three different temperatures. The three pressures studied were 117.5 torr, 326.5 torr and 461.0 torr, the run pressure being read from the mercury manometer. The three temperatures used were -76.5° C., -63.5° C., and -45.3° C. The -76.5° C. temperature was achieved by a dry ice-isopropanol bath circulated by a stirrer. The bath was contained in a large insulated tank wich held all eight sample tubes. Wire screening was used to prevent direct contact of the glass sample tube

with pieces of the dry ice. Fresh dry ice was added as required, about every four to six hours. The rate of $CO_2$ sorption was followed for about 30 hours per experiment, the temperature remaining constant at $-76.5 \pm 0.5^{\circ}$ C., as read by a vapor pressure thermometer charged with ammonia. The rate of uptake was found to be so slow that the zero point reading on the wall chart was made after the dose of gas had been admitted. This introduced no significant error and made a buoyancy correction unnecessary. The sorption rate was followed every ten minutes for the first hour, every 30 minutes for the second and third hours, every 60 minutes for the fourth, fifth and sixth hours, and every two hours for the remainder of the run. As the $CO_2$ was sorbed, it was replenished, maintaining run pressure throughout the experiment to $\pm$ 1 torr.

The $-63.5^{\circ}$ C. temperature was achieved by using a chloroform slush bath held in a dewar flask. The slush was regenerated every two hours by freezing with liquid nitrogen, maintaining the temperature within $\pm 0.2^{\circ}$ C. as read by a vapor pressure thermometer. A tubular glass sleeve open at both ends was placed around the sample tube to prevent direct contact of the tube with the liquid nitrogen added to regenerate the slush. If liquid nitrogen did make direct contact with the sample tube, it caused freezing out of the $CO_2$ and a consequent pressure drop. Except for temperature, this series of runs and those at $-45.3^{\circ}$ C. were identical to those at $-76.5^{\circ}$ C.

The -45.3° C. temperature was maintained by a chlorobenzene slush bath which also was regenerated every two hours. Temperature control was within ± 0.2° C. Each combination of run conditions was repeated and the data was successfully reproduced within experimental error.

Sorption at the three temperatures just discussed was much too slow to effectively measure equilibrium isotherms. In some cases extrapolation of the rate curve did allow the equilibrium value to be estimated, and for a few samples, sorption had essentially ceased by the end of the rate run for the highest temperature. In an attempt to achieve equilibrium isotherms, runs were made at 0° C. using an ice-water mixture and at 25° C. using a controlled temperature water bath. Even at these temperatures, only two of the samples achieved equilibrium within a reasonable time. These were sample 1, the oleoresinous film and sample 8, the hydrocarbon B film. All others were still gaining some weight after 24 hours, especially sample 2, the phenolic film, whose rate of uptake was slowest in all runs with $CO_2$.

Oxygen Sorption

The sorbate source was U. S. P. grade compressed oxygen. It was purified by passing it through an ascarite tube and two traps at dry ice temperature. It was then collected with liquid nitrogen in a

trap that was subsequently isolated from the rest of the purification train. The trap was outgassed three times for two minutes each time, after which the oxygen displayed the correct vapor pressure at liquid nitrogen temperature. At that point the oxygen was assumed to be free of any non-condensible gases and was allowed to expand into the storage bulb. Two runs were attempted, one at liquid nitrogen temperature and one at 25° C. In both cases no sorption could be detected; the only spring movement was in the weight lost direction caused by buoyancy effects.

Water Vapor Sorption

The rate of water vapor sorption and desorption was investigated at two pressures, 4.7 torr and 6.8 torr, at 25.0° C. Desorption curves were possible as equilibrium was easily achieved. Sorption was so fast that only one sample tube at a time could be studied and in some cases only the desorption curves furnished data covering the initial stages of the process. The temperature was controlled with a constant temperature water bath maintained to $\pm$ 0.1° C. and the water vapor pressure was read with an oil manometer. The procedure was identical to that used in the $CO_2$ studies with the exception that data was taken every 30 seconds at first, the periods gradually lengthening to ten minutes as the sorption or desorption process slowed down. For sorption a zero reading was made before sorbate

addition since water uptake was so rapid. This was satisfactory since the pressures used were so small that buoyancy corrections were negligible. Desorption runs were started only after equilibrium was achieved. At that point the vapor in the system was frozen with liquid nitrogen, producing a vacuum lower than $10^{-3}$ torr. Desorption was then followed versus time. This technique evacuated the sample with a minimum of spring upset in a period of a few seconds.

## X-ray Diffraction

X-ray diffraction patterns of the films were determined to see what degree of crystallinity they possessed. The patterns of the eight films were compared with that of a film of polyethylene, which is known to be relatively crystalline. X-ray data was taken using a General Electric XRD-5 X-ray diffraction instrument with copper $K_{\alpha}$ radiation. The horizontal tube and spectrogoniometer were used so diffraction peaks were traced out directly on chart paper. Several thicknesses of the films were mounted on glass slides and used directly in the sample holder of the spectrogoniometer.

# EXPERIMENTAL RESULTS AND CALCULATIONS

## Sorption of Carbon Dioxide

The sorption rate curves of carbon dioxide on the eight organic films were all of similar shape. Table II lists the $CO_2$ runs made and conditions used. Listed also are the equilibrium sorption values for those cases where equilibrium was obtained or where it was possible to extrapolate the rate curve to the equilibrium value. It is seen that no samples approached equilibrium at -76.5° C. and that sample 2 did not achieve equilibrium at any temperature studied. The plots shown in Figure 4 are representative of the data obtained. Two identical runs are plotted to show the degree of reproducibility. As the temperature was raised the general trend was for faster rates but less overall uptake of gas as is seen in Figure 5 for sample 1. Total amount sorbed increased with pressure in all cases.

For the five samples where equilibrium sorption values were available at both -63.5 and -45.3° C., isotherm plots were drawn and isosteric heats were calculated. Figure 6 shows two typical isotherms for sample 1. Equation 7 was used for the calculations. The required pressures at the two different temperatures were read from the isotherm plots at positions corresponding to a constant amount sorbed. Table III summarizes the results of these

Table II. Sorption runs with $CO_2$ on organic films.

| Temp., °C. | $CO_2$ Press., Torr | Run No. | Equilibrium sorption value, mg./g. Sample No. 1 | 2 | 3 | 4 | 5 | 6 | 7 | 8 |
|---|---|---|---|---|---|---|---|---|---|---|
| -76.5 | 117.5 | $CO_2$-23, 24, 25 | ---- | ---- | ---- | ---- | ---- | ---- | ---- | ---- |
| | 326.5 | $CO_2$-26, 28 | ---- | -- | ---- | ---- | ---- | ---- | ---- | ---- |
| | 461.0 | $CO_2$-27, 29 | ---- | -- | ---- | ---- | ---- | ---- | ---- | ---- |
| -63.5 | 117.0 | $CO_2$-30, 34 | 9.7 | -- | ---- | 11.0 | 7.2 | ---- | 14.8 | 14.6 |
| | 326.5 | $CO_2$-31, 35 | 16.8 | -- | ---- | 18.0 | 13.0 | ---- | 25.8 | 24.4 |
| | 461.0 | $CO_2$-32, 33 | 19.7 | -- | ---- | 21.8 | 16.0 | ---- | 31.2 | 28.6 |
| -45.3 | 117.5 | $CO_2$-36, 39 | 5.0 | -- | 7.4 | 6.0 | 4.0 | 4.9 | 9.5 | 7.5 |
| | 326.5 | $CO_2$-37, 40 | 9.0 | -- | 13.6 | 11.0 | 7.3 | 8.6 | 15.8 | 13.4 |
| | 461.0 | $CO_2$-38, 41 | 10.8 | -- | 16.4 | 13.3 | 8.7 | 10.0 | 19.2 | 15.1 |
| 0 | 117.5 | $CO_2$-43 | 0.4 | -- | 1.3 | 1.2 | 0.6 | 1.7 | 2.0 | 1.0 |
| 25 | Up to 817.5 | $CO_2$-44 | Attempt at complete isotherm. | | | | | | | |

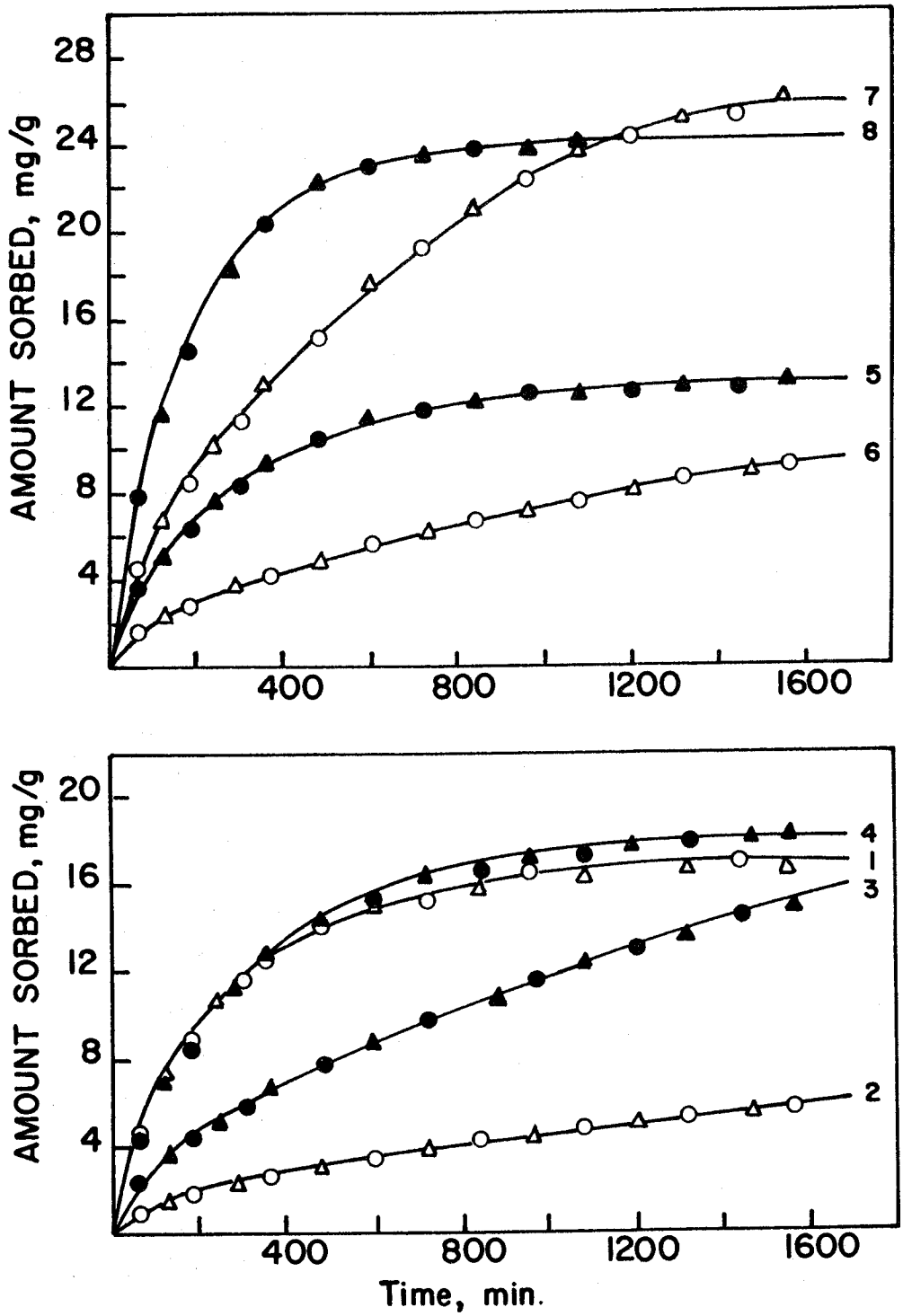


FIGURE 4. RATE OF $CO_2$ SORPTION ON THE EIGHT ORGANIC FILMS, RUNS $CO_2$-31, 35

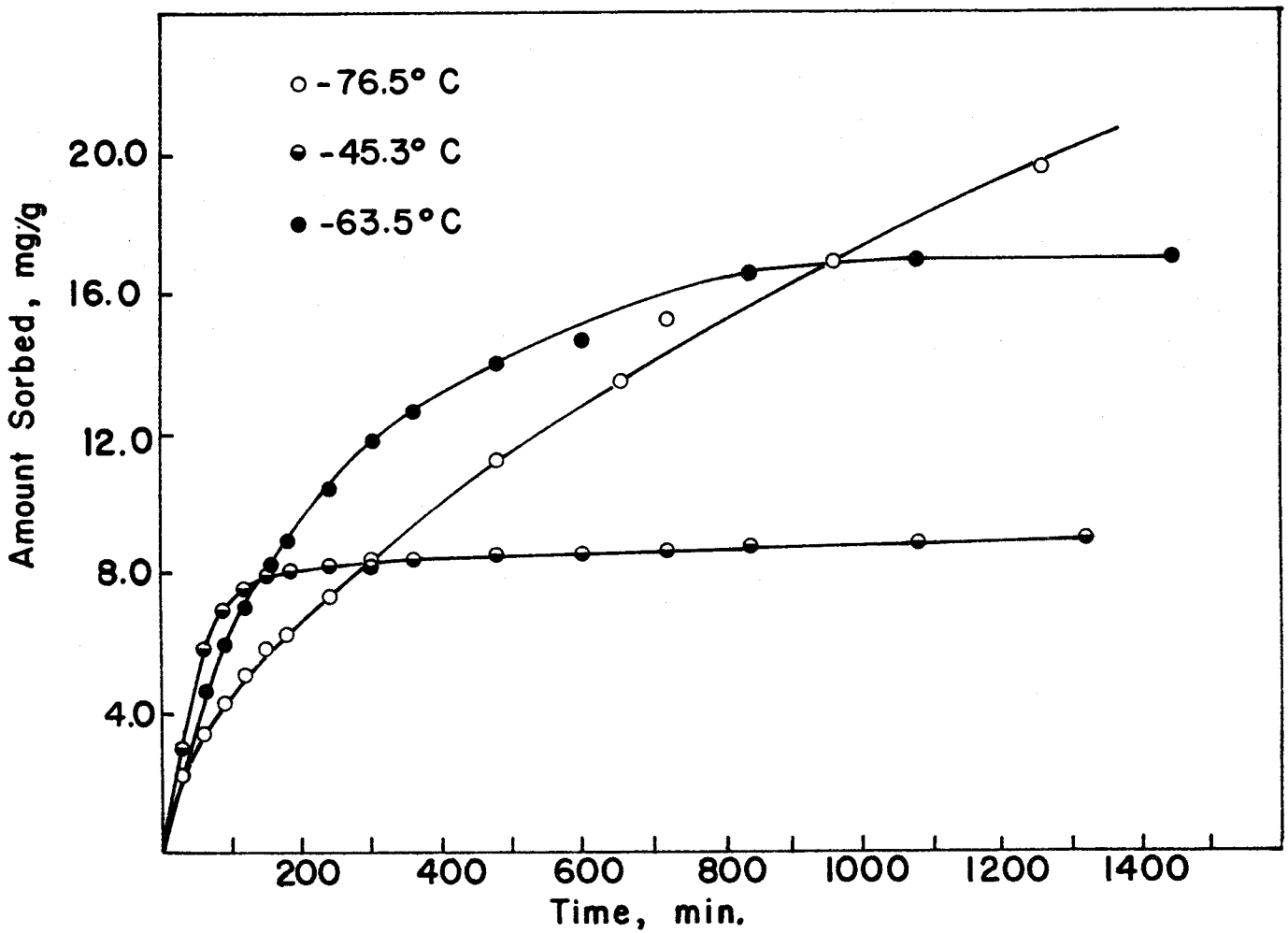


FIGURE 5. TEMPERATURE EFFECT ON RATE OF SORPTION OF $CO_2$ ON SAMPLE I AT 326.5 TORR.

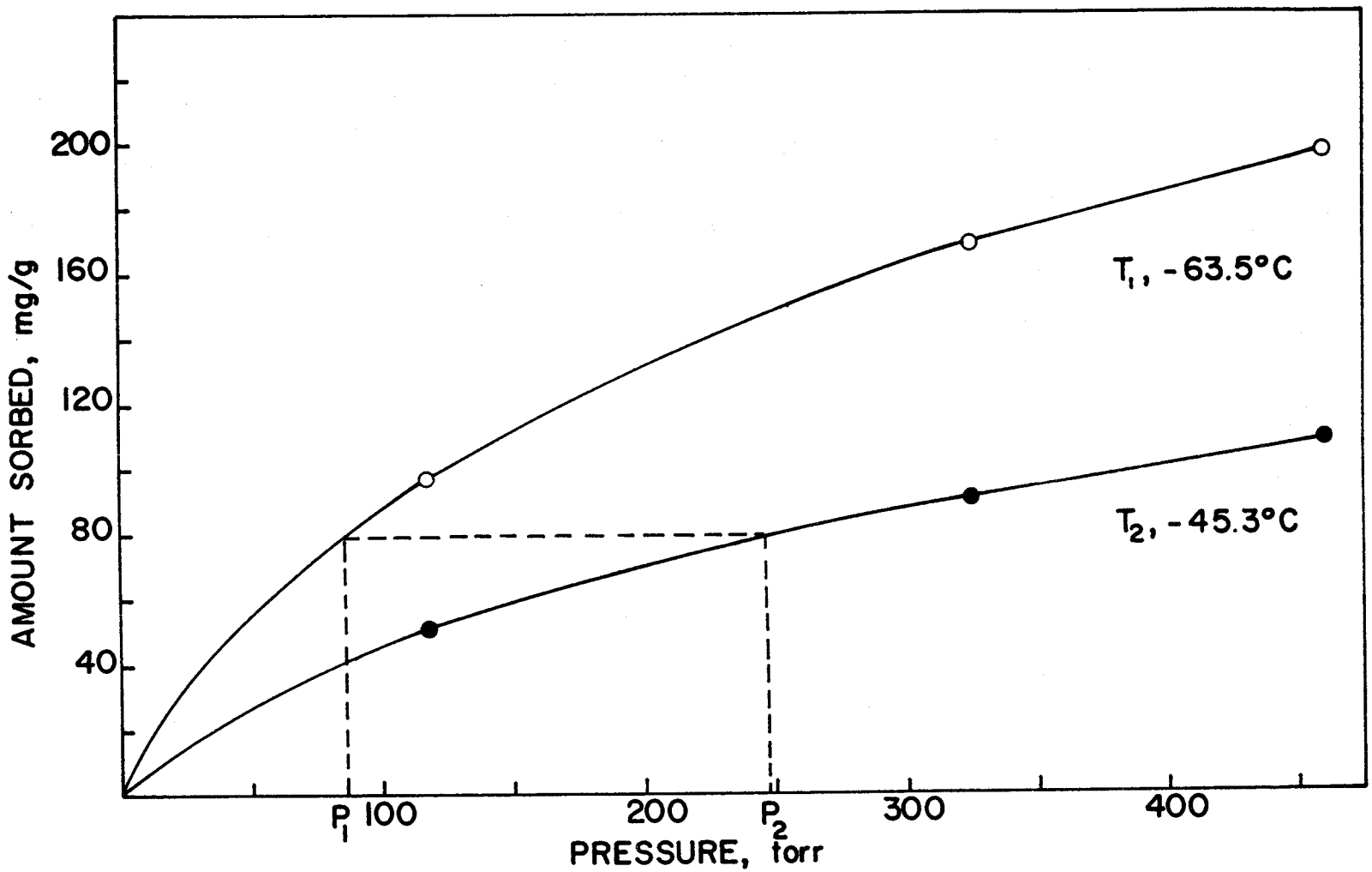


FIGURE 6. ISOTHERM PLOTS FOR SAMPLE I, USED TO CALCULATE ISOTERIC HEATS

calculations. No attempt was made to fit the equilibrium data to a theoretical isotherm due to the small number of values available.

Table III. Isosteric heats of sorption for $CO_2$ on organic films between -45.3 and -63.5° C.

| Sample No. | Isosteric heat, kcal/mole, Amount sorbed, mg/g. | | | | | | | | | |
|---|---|---|---|---|---|---|---|---|---|---|
| | 2 | 4 | 6 | 8 | 10 | 12 | 14 | 16 | 18 | 20 |
| 1 | 3.2 | 4.1 | 4.8 | 5.5 | 6.1 | --- | --- | --- | --- | --- |
| 4 | 4.7 | 4.4 | 4.5 | 4.8 | 5.2 | 5.5 | 5.4 | --- | --- | --- |
| 5 | 3.4 | 3.8 | 4.7 | 5.5 | --- | --- | --- | --- | --- | --- |
| 7 | 2.8 | 2.8 | 2.8 | 2.9 | 3.2 | 3.6 | 4.2 | 4.7 | 4.8 | 4.6 |
| 8 | 4.8 | 4.7 | 4.8 | 4.9 | 5.2 | 5.6 | 6.2 | --- | --- | --- |

$\Delta H$ sublimation for $CO_2$ at -56.2° C. is 5.8 kcal/mole.

## Kinetic Calculations

### Chemisorption

A previous investigation (20) had interpreted the rate effect of the $CO_2$ interaction on the basis of activated chemisorption. Proceeding from this premise, the rate data from runs $CO_2$-23 through $CO_2$-41 were tested with the empirical Elovich equation (Equation 8). The rate curves were plotted on large graph paper and the curves smoothed out. Then values were read from the plots to two decimal

places for amount sorbed corresponding to 30 minute intervals throughout the length of the run.

To test the Elovich equation, the method of Sarmousakis and Low (24) was used, as previously described. The calculations were programmed for the IBM-7090 computer. This method calculates the Elovich parameters at various times along the rate curve and the constancy of the parameters throughout an experiment is a measure of the degree to which the equation fits the data. Tables IV and V summarize the results of these calculations. For runs at -76.5° C., where the rate is slowest and thus the experimental accuracy the greatest, the average deviation during any single experiment varied from $\pm$ 5 to $\pm$ 10 percent for both $\underline{a}$ and $\alpha$. For the higher temperature runs the deviations were somewhat greater. It was mentioned in the discussion of theory that when the Elovich equation is used in its integrated form (Equation 10), a plot of the amount sorbed, q, versus log $(t+t_o)$ provides a test of this equation. It was further seen that $t_o$ was equal to $1/\underline{a}\alpha$ (Equation 11). Usually $t_o$ is derived by trial and error and $\underline{a}$ and $\alpha$ are calculated from the Elovich plot (q versus $(t+t_o)$). However, if $\underline{a}$ and $\alpha$ are already known, $t_o$ may be calculated directly and the Elovich plot can be used as a secondary check on whether the original calculations of $\underline{a}$ and $\alpha$ were valid. This was done and the $t_o$ values are listed in Table VI.

Table IV. Values of a from Elovich equation, $CO_2$ on organic films.

| Temp., °C. | Press., Torr | a, mg/g-min. Sample No. 1 | 2 | 3 | 4 | 5 | 6 | 7 | 8 |
|---|---|---|---|---|---|---|---|---|---|
| | 117.5 | 0.015 | 0.0035 | 0.0088 | 0.013 | 0.011 | 0.0040 | 0.015 | 0.024 |
| -76.5 | 326.5 | 0.030 | 0.0063 | 0.016 | 0.034 | 0.023 | 0.0082 | 0.024 | 0.064 |
| | 461.0 | 0.037 | 0.0072 | 0.018 | 0.046 | 0.024 | 0.0074 | 0.026 | 0.076 |
| | 117.5 | 0.040 | 0.0062 | 0.0094 | 0.044 | 0.022 | 0.0066 | 0.023 | 0.072 |
| -63.5 | 326.5 | 0.096 | 0.0086 | 0.020 | 0.094 | 0.062 | 0.014 | 0.050 | 0.16 |
| | 461.0 | 0.11 | 0.0095 | 0.025 | 0.11 | 0.090 | 0.016 | 0.058 | 0.22 |
| | 117.5 | 0.10 | 0.0067 | 0.022 | 0.088 | 0.060 | 0.024 | 0.062 | 0.18 |
| -45.3 | 326.5 | 0.20 | 0.012 | 0.046 | 0.22 | 0.14 | 0.051 | 0.15 | 0.38 |
| | 461.0 | 0.25 | 0.016 | 0.065 | 0.28 | 0.23 | 0.063 | 0.18 | 0.35 |

Table V. Values of $\alpha$ from Elovich equation, $CO_2$ on organic films.

| Temp., °C. | Press., Torr | $\alpha$, g./mg. Sample No. 1 | 2 | 3 | 4 | 5 | 6 | 7 | 8 |
|---|---|---|---|---|---|---|---|---|---|
| | 117.5 | 0.12 | 0.42 | 0.28 | 0.14 | 0.18 | 0.32 | 0.13 | 0.073 |
| -76.5 | 326.5 | 0.064 | 0.36 | 0.13 | 0.66 | 0.093 | 0.28 | 0.050 | 0.045 |
| | 461.0 | 0.050 | 0.28 | 0.079 | 0.48 | 0.063 | 0.17 | 0.028 | 0.033 |
| | 117.5 | 0.21 | 0.68 | 0.18 | 0.24 | 0.30 | 0.26 | 0.098 | 0.16 |
| -63.5 | 326.5 | 0.15 | 0.28 | 0.094 | 0.14 | 0.16 | 0.16 | 0.062 | 0.096 |
| | 461.0 | 0.12 | 0.22 | 0.072 | 0.12 | 0.16 | 0.14 | 0.047 | 0.082 |
| | 117.5 | 0.56 | 0.46 | 0.31 | 0.40 | 0.65 | 0.54 | 0.26 | 0.50 |
| -45.3 | 326.5 | 0.23 | 0.24 | 0.16 | 0.26 | 0.32 | 0.30 | 0.17 | 0.19 |
| | 461.0 | 0.16 | 0.20 | 0.14 | 0.22 | 0.32 | 0.26 | 0.12 | 0.11 |

Table VI. Values of $t_o$ back-calculated from the Elovich parameters, $CO_2$ on organic films.

| Temp., °C. | Press., Torr | $t_o$, min. Sample No. 1 | 2 | 3 | 4 | 5 | 6 | 7 | 8 |
|---|---|---|---|---|---|---|---|---|---|
| | 117.5 | 556 | 680 | 406 | 549 | 505 | 781 | 513 | 571 |
| -76.5 | 326.5 | 521 | 440 | 481 | 445 | 468 | 436 | 833 | 347 |
| | 461.0 | 541 | 496 | 703 | 453 | 661 | 795 | 1373 | 399 |
| | 117.5 | 119 | 237 | 591 | 95 | 152 | 583 | 444 | 87 |
| -63.5 | 326.5 | 69 | 415 | 532 | 76 | 101 | 446 | 323 | 65 |
| | 461.0 | 76 | 478 | 556 | 76 | 69 | 446 | 367 | 55 |
| | 117.5 | 18 | 324 | 147 | 284 | 26 | 77 | 62 | 11 |
| -45.3 | 326.5 | 22 | 347 | 136 | 175 | 22 | 65 | 39 | 14 |
| | 461.0 | 25 | 312 | 110 | 162 | 14 | 61 | 46 | 26 |

Figure 7 shows the Elovich plot behavior obtained with sample 1 at three temperatures and constant pressure. Straight line sections are obtained with abrupt discontinuities appearing at the higher temperatures. Other samples gave similar behavior.

Activation energies of sorption were calculated from the Arrhenius equation modified by substituting $\ln (t_1/t_2)$ for $\ln k$ of Equation 22, where $t_1/t_2$ is the ratio of times required for the sorption of a given amount of gas. Thus the equation takes the form:

$$\ln (t_1/t_2) = \frac{E_a}{2.303\ R} \left[\frac{T_2 - T_1}{T_1 T_2}\right] \qquad [40]$$

The results of these calculations between -63.5 and -76.5° C. are given in Table VII.

Values of the activation energy between -45.3 and -63.5° C. were calculated for a few of the samples where sufficient data were available and the results were very similar, corresponding values being slightly smaller than those at the lower temperature range.

Table VII. Activation energies for rate of sorption of $CO_2$ on organic films between -63.5 and -76.5° C.

| Sample No. | Press., Torr | Activation Energy, kcal./mole — Amount sorbed, mg./g. | | | | | | | | | | | | |
|---|---|---|---|---|---|---|---|---|---|---|---|---|---|---|
| | | 2 | 4 | 6 | 8 | 10 | 12 | 14 | 16 | 18 | 20 | 22 | 24 | 26 |
| 1 | 117.5 | --- | 2.6 | 2.8 | 1.7 | --- | --- | --- | --- | --- | --- | --- | --- | --- |
| | 326.5 | --- | 2.4 | 3.6 | 4.1 | 4.0 | 3.4 | 2.4 | --- | --- | --- | --- | --- | --- |
| | 461.0 | --- | 2.8 | 4.6 | 4.0 | 4.0 | 3.8 | 3.5 | 3.0 | 1.3 | --- | --- | --- | --- |
| 2 | 117.5 | 2.0 | --- | --- | --- | --- | --- | --- | --- | --- | --- | --- | --- | --- |
| | 326.5 | 3.8 | 3.6 | --- | --- | --- | --- | --- | --- | --- | --- | --- | --- | --- |
| | 361.0 | 3.4 | 3.3 | --- | --- | --- | --- | --- | --- | --- | --- | --- | --- | --- |
| 3 | 117.5 | 3.6 | 3.4 | --- | --- | --- | --- | --- | --- | --- | --- | --- | --- | --- |
| | 326.5 | --- | 2.7 | 3.0 | 3.1 | 3.1 | --- | --- | --- | --- | --- | --- | --- | --- |
| | 461.0 | --- | 2.7 | 3.0 | 2.9 | 3.0 | 2.8 | 2.8 | --- | --- | --- | --- | --- | --- |
| 4 | 117.5 | --- | 3.2 | 3.6 | 3.0 | 1.6 | --- | --- | --- | --- | --- | --- | --- | --- |
| | 326.5 | --- | 2.1 | 2.9 | 3.1 | 2.9 | 2.6 | 2.0 | 1.0 | --- | --- | --- | --- | --- |
| | 461.0 | --- | 1.2 | 2.3 | 2.8 | 3.0 | 2.8 | 2.5 | 2.0 | 1.3 | --- | --- | --- | --- |
| 5 | 117.5 | 1.3 | 2.0 | 0.8 | --- | --- | --- | --- | --- | --- | --- | --- | --- | --- |
| | 326.5 | --- | 2.8 | 2.6 | 2.6 | 2.3 | 0.7 | --- | --- | --- | --- | --- | --- | --- |
| | 461.0 | --- | 3.5 | 4.1 | 4.2 | 3.8 | 3.2 | 2.0 | --- | --- | --- | --- | --- | --- |
| 6 | 117.5 | 4.8 | --- | --- | --- | --- | --- | --- | --- | --- | --- | --- | --- | --- |
| | 326.5 | 5.6 | 5.3 | --- | --- | --- | --- | --- | --- | --- | --- | --- | --- | --- |
| | 461.0 | 5.3 | 5.9 | 5.8 | --- | --- | --- | --- | --- | --- | --- | --- | --- | --- |
| 7 | 117.5 | --- | 2.8 | 3.1 | 3.2 | 3.3 | 3.3 | --- | --- | --- | --- | --- | --- | --- |
| | 326.5 | --- | --- | 3.2 | 3.2 | 3.2 | 3.3 | 3.2 | 3.2 | 3.3 | 3.3 | 3.1 | --- | --- |
| | 461.0 | --- | --- | 3.1 | 3.3 | 3.4 | 3.5 | 3.4 | 3.3 | 3.4 | 3.3 | 3.3 | 3.2 | 3.0 |
| 8 | 117.5 | 5.5 | 3.4 | 2.7 | 2.5 | 2.4 | 1.9 | --- | --- | --- | --- | --- | --- | --- |
| | 326.5 | --- | --- | 1.0 | 2.2 | 2.7 | 3.0 | 3.1 | 2.9 | 2.6 | 2.0 | 1.0 | --- | --- |
| | 461.0 | --- | --- | 2.6 | 2.8 | 3.0 | 3.1 | 3.2 | 3.1 | 3.0 | 2.8 | 2.6 | 2.2 | 1.2 |

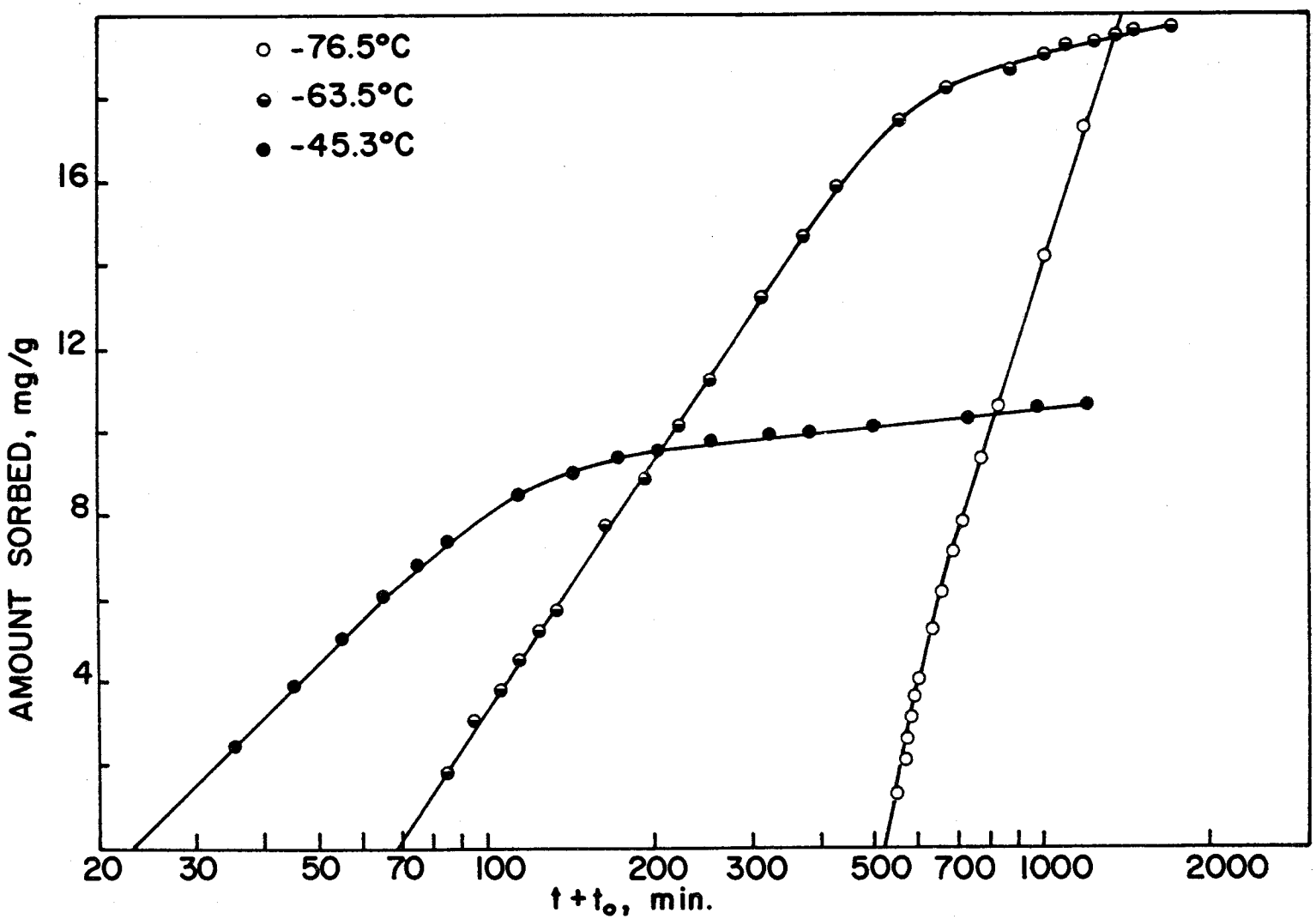


FIGURE 7. ELOVICH PLOTS FOR $CO_2$ SORPTION ON SAMPLE I AT 461.0 TORR

Diffusion

A second possible interpretation to explain a rate effect in sorption is that a slow diffusion process is taking place. With this thought in mind, the rate data for $CO_2$ on the eight organic films were treated by diffusion theory. Referring to Equations 27 and 31, it is seen that if Fickian diffusion is taking place, the reduced sorption curve, a plot of $q/q_e$ versus $\sqrt{t}/L$, should give a straight line. The relative amount sorbed, $q/q_e$, is the ratio of the amount sorbed at any particular time to the equilibrium amount, and $\sqrt{t}/L$ is a ratio of the square root of time to the film thickness. Reduced sorption curves were plotted for runs $CO_2$-23 through $CO_2$-41. Figure 8 shows a few representative curves for sample 1 at three temperatures and constant pressure. In cases where the equilibrium value of amount sorbed was not reached, the instantaneous amount sorbed was plotted versus $\sqrt{t}/L$. The overall shape of the curve in this case will be the same, linearity still being achieved if diffusion is taking place.

All reduced sorption curves for $CO_2$ showed long sections of linearity but deviated from linearity near the origin. Thus the initial slope could not be used to calculate diffusion coefficients. However, the linear portion of the plots extended through $q/q_e$ equal to 0.5 in all cases. Therefore, Equation 36 was used to calculate an average

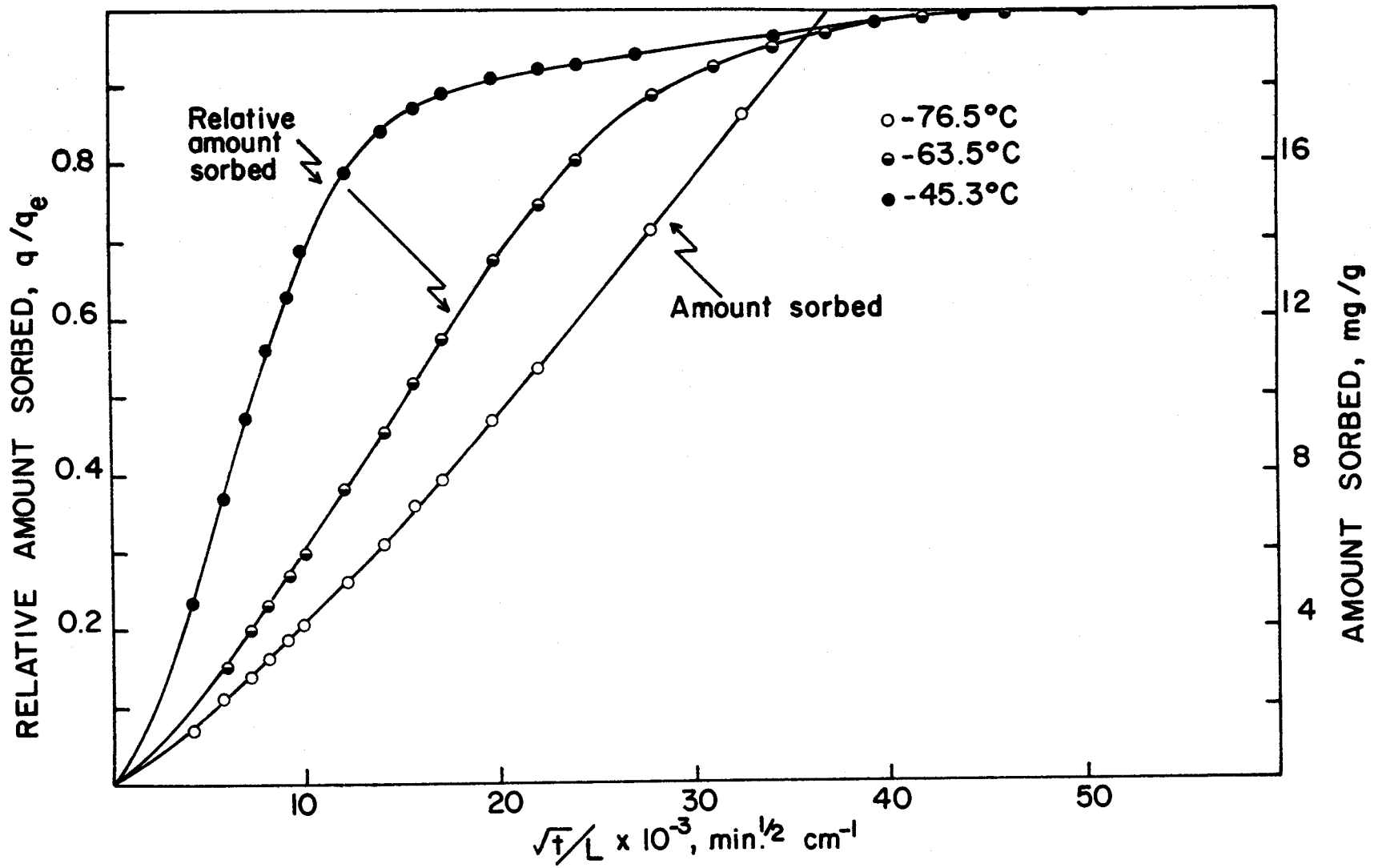


FIGURE 8. REDUCED SORPTION CURVES FOR $CO_2$ SORPTION ON SAMPLE I AT 461.0 TORR.

sorption coefficient, $\overline{R}_s$. The results of these sorption coefficient calculations are collected in Table VIII. Listed also are the limiting diffusion coefficients, $D_o$, obtained by extrapolating the pressure dependent $\overline{R}_s$ values to zero $CO_2$ activity. In the cases where the equilibrium value of amount sorbed was not known, the slope of the curve q versus $\sqrt{t}/L$ is given in parentheses instead of $\overline{R}_s$. The square of this slope is roughly proportional to the sorption coefficient since deviation from Fickian diffusion was slight, and thus trends can still be seen. An overall average precision for these determinations was $\pm 3.5$ percent.

Using Equation 38 in the definite integral form and the $D_o$ values from Table VIII, activation energies for the diffusion process were calculated. These are tabulated in Table IX.

Table VIII. Values of the average sorption coefficients, $\bar{R}_s$, and limiting diffusion coefficients, $D_o$, $CO_2$ on organic films.

| Temp., °C. | Press., Torr | $\bar{R}_s$ and $D_o \times 10^{12}$, cm.$^2$/sec. * | | | | | | | |
|---|---|---|---|---|---|---|---|---|---|
| | | Sample No. | | | | | | | |
| | | 1 | 2 | 3 | 4 | 5 | 6 | 7 | 8 |
| -76.5 | 461.0 | (10.33) | (2.07) | (6.87) | (8.20) | (7.17) | (2.20) | (12,87) | (20.38) |
| | 326.5 | (7.93) | (1.73) | (5.27) | (6.13) | (5.70) | (1.78) | (9.38) | (16.50) |
| | 117.5 | (4.03) | (0.995) | (2.53) | (2.77) | (2.80) | (1.03) | (4.63) | (7.78) |
| -63.5 | 461.0 | 3.48 | (2.68) | (9.00) | 1.47 | 2.93 | (3.67) | 1.82 | 5.57 |
| | 326.5 | 3.20 | (2.22) | (6.90) | 1.34 | 2.70 | (2.97) | 1.68 | 4.90 |
| | 117.5 | 2.40 | (1.27) | (3.30) | 0.917 | 1.90 | (1.62) | 1.39 | 3.52 |
| | $D_o$ | 1.08 | ----- | ----- | 0.35 | 0.74 | ----- | 0.66 | 1.55 |
| -45.3 | 117.5 | 15.12 | (3.65) | 3.68 | 4.77 | 12.15 | 2.60 | 7.50 | 23.07 |
| | 326.5 | 13.60 | (2.93) | 3.48 | 4.73 | 10.20 | 2.40 | 6.13 | 18.52 |
| | 461.0 | 9.77 | (1.53) | 2.68 | 3.23 | 7.72 | 1.90 | 4.22 | 11.08 |
| | $D_o$ | 4.17 | ---- | 1.26 | 1.05 | 3.90 | 0.91 | 1.98 | 3.90 |

* Numbers in parentheses are just the slope of the curve q versus $\sqrt{t}/L$.
$\bar{R}_s$ values could not be calculated as equilibrium sorption values were not known.

Table IX. Activation energies for rate of diffusion of $CO_2$ in organic films between -45.3 and -63.5° C.

| Sample No. | Activation energy, kcal/mole |
|---|---|
| 1 | 7.0 |
| 2 | --- |
| 3 | --- |
| 4 | 5.7 |
| 5 | 8.7 |
| 6 | --- |
| 7 | 5.7 |
| 8 | 4.8 |

## Sorption of Water Vapor

Two runs were made to get comparative data on the rate of water vapor sorption. The rate of interaction was very fast and apparently non-Fickian. Initial portions of the reduced sorption curves, however, were not well defined as the sorption was so fast that one-fourth to one-half of the process was over before the first reading could be taken. The largest experimental problem in this regard was that the springs bounced up and down from the surge of vapor into or out of the sample tube at time zero. Twenty to forty seconds would elapse before stability was achieved in sorption but somewhat better results were achieved in desorption. Both sorption coefficients, $\bar{R}_s$, and desorption coefficients, $\bar{R}_d$, were calculated from the time values at $q/q_e = 0.5$ using Equation 36. These results are tabulated in Table X.

Table X. Values for average sorption and desorption coefficients, $\bar{R}_s$ and $\bar{R}_d$, $H_2O$ on organic films at 25.0° C.

| Sample No. | Press., Torr | $\bar{R}_s \times 10^{12}$, $cm.^2/sec.$ | $\bar{R}_d \times 10^{12}$, $cm.^2/sec.$ |
|---|---|---|---|
| 1 | 6.8 | 711 | 405 |
| | 4.7 | 592 | 227 |
| 2 | 6.8 | 26.1 | 22.7 |
| | 4.7 | 33.6 | 19.6 |
| 3 | 6.8 | 2420 | 1000 |
| | 4.7 | 1680 | 848 |
| 4 | 6.8 | --- | 237 |
| | 4.7 | 766 | 71.4 |
| 5 | 6.8 | 340 | 419 |
| | 4.7 | 480 | 218 |
| 6 | 6.8 | 105 | 59.9 |
| | 4.7 | 106 | 33.9 |
| 7 | 6.8 | 405 | 250 |
| | 4.7 | 445 | 246 |
| 8 | 6.8 | 1680 | 766 |
| | 4.7 | 1680 | 694 |

## X-Ray Diffraction

The X-ray measurements were very qualitative, being made only to see if some of the films exhibited crystallinity. A polyethylene film was used as a standard. Table XI summarizes the information obtained.

Table XI. X-ray diffraction patterns of the organic films.

| Sample | Comments on Diffraction Patterns |
|---|---|
| Polyethylene | Relatively sharp peak at 4.13 Å. |
| 1 | Series of small peaks ranging from 1.04 to 1.82 Å. |
| 2 | Very weak pattern between 2.56 and 5.21 Å. |
| 3 | No diffraction detected. |
| 4 | Same film as 3, no diffraction detected. |
| 5 | Medium intense peaks from 1.00 to 1.10 Å and from 1.56 to 2.01 Å. |
| 6 | Very weak pattern between 1.02 and 1.26 Å. |
| 7 | No diffraction detected. |
| 8 | Very diffuse pattern over wide range. |

# DISCUSSION

## Sorption Rates and Type of Interaction

The major problem in this investigation was to elucidate the mechanism of interaction of carbon dioxide with the eight organic films. A previous investigation by Patterson (20) indicated that the interaction was an activated chemisorption process. Patterson made this tentative conclusion on the basis of investigations mostly made on sample 1 and the data available to him was limited. He concluded that the process was chemisorption primarily on the basis that his data fit an Elovich plot, q versus log $(t+t_o)$, where he obtained $t_o$ by trial and error. His values for this parameter were mostly on the order of 500 minutes. The present study resulted in sufficient data to thoroughly test the Elovich equation. Especially helpful was that a mathematical analysis could be used, precluding the necessity of obtaining trial and error values of $t_o$.

Referring to Tables IV and V, it can be seen that the normally obtained temperature and pressure dependence of the Elovich parameter, a, was found. That is, a for all samples increased markedly with both temperature and pressure. The variations of $\alpha$ however are seen to be somewhat anomalous. Indeed, $\alpha$ does decrease with pressure, but rather strongly. As previously mentioned, it should decrease with pressure, but only slightly since the slow adsorption

rate is believed to be dependent only on the concentration of surface sites. It could be possible, however, that the initial gas pressure first coming in contact with the surface exerts a relatively strong influence on the instantaneous production of these surface sites. The temperature variation of $\alpha$, however, is seen to be very erratic. Low (17) states that the temperature coefficient of $\alpha$ may be positive or negative depending on the gas-solid system. Examination of Table V shows $\alpha$ to increase consistantly with temperature for samples 1, 5 and 8, to decrease for sample 2 and to vary randomly for the other four samples. Variation of the temperature coefficient between the eight samples would be expected as their surfaces are no doubt considerably different in nature. However, the erratic up and down nature of one-half of the samples studied can only be explained on the basis that a complete transition of type of interaction is taking place. This seems highly unlikely for these samples and no other evidence was found to support this view. According to Low the temperature variations of the Elovich parameters are so poorly understood that any rigorous correlation of properties with these temperature coefficients is impossible.

Elovich plots were made using back-calculated $t_o$ values. Table VI shows that most of these $t_o$ values are in the hundreds of minutes, in agreement with the work of Patterson. The Elovich plots seen in Figure 7 do show linear regions but abrupt changes in

slope are in evidence, corresponding to the times when sorption had slowed down markedly. Although linear segments were obtained, a question can be raised with regard to arbitrarily adding a value to the time which is itself much larger than the actual time measured during most of the experiment. Almost any log plot could be straightened by adding large enough numbers to the values from which the logarithms are derived. The $t_o$ values shown in Table VI correspond to times during which 50 to 75 percent of the sorption has already taken place. Such a procedure is certainly open to criticism.

The fit of the $CO_2$ rate data to the Elovich equation did not conclusively rule out a chemisorption process but it certainly did cast some doubt on the validity of such an interpretation. Consequently, the data were tested for the occurrence of a diffusion process. Theory states that the amount sorbed plotted against the square root of time should give a straight line over most of the course of the experiment, leveling out at large times as the process terminates. As Figure 8 demonstrates, extended straight line portions are indeed found in these reduced sorption curves, covering 60 to 75 percent of the amount sorbed.

Examination of these reduced sorption curves together with the Elovich plots resulted in a striking comparison. If one looks at q plotted against either log $(t+t_o)$ or $\sqrt{t}/L$, very similarly shaped

curves are obtained, the breaks occurring at the same actual experimental times. This is demonstrated in Figure 9 for sample 1. This figure is simply a comparison between Figures 7 and 8, the only change being that the abscissa for Figure 8 is changed from $q/q_e$ to q so that it will be consistent with Figure 7. This similarity was seen in all samples throughout the range of conditions studied. What this means is that treatment by both theories has reduced the data to roughly the same condition. In the case of diffusion, direct data points are used, the only modification being that the square root of time is plotted instead of time directly. For the Elovich treatment, a constant added to the time was required, the size of which casts some doubt on the technique.

To obtain more insight into the mechanism of sorption of $CO_2$, activation energies assuming both a chemisorption process and a diffusion process were calculated. Isosteric heats of sorption were also calculated in all cases where equilibrium sorption values were known. The activation energies listed in Table VII were much smaller than the values calculated by Patterson (20) but this can be explained by the fact that he based his calculation on constant amount sorbed at various relative pressures while the values listed here are calculated on the basis of constant amount sorbed at various absolute pressures. Although the values for the activation energy of diffusion from Table IX are seen to be larger than those for chemisorption,

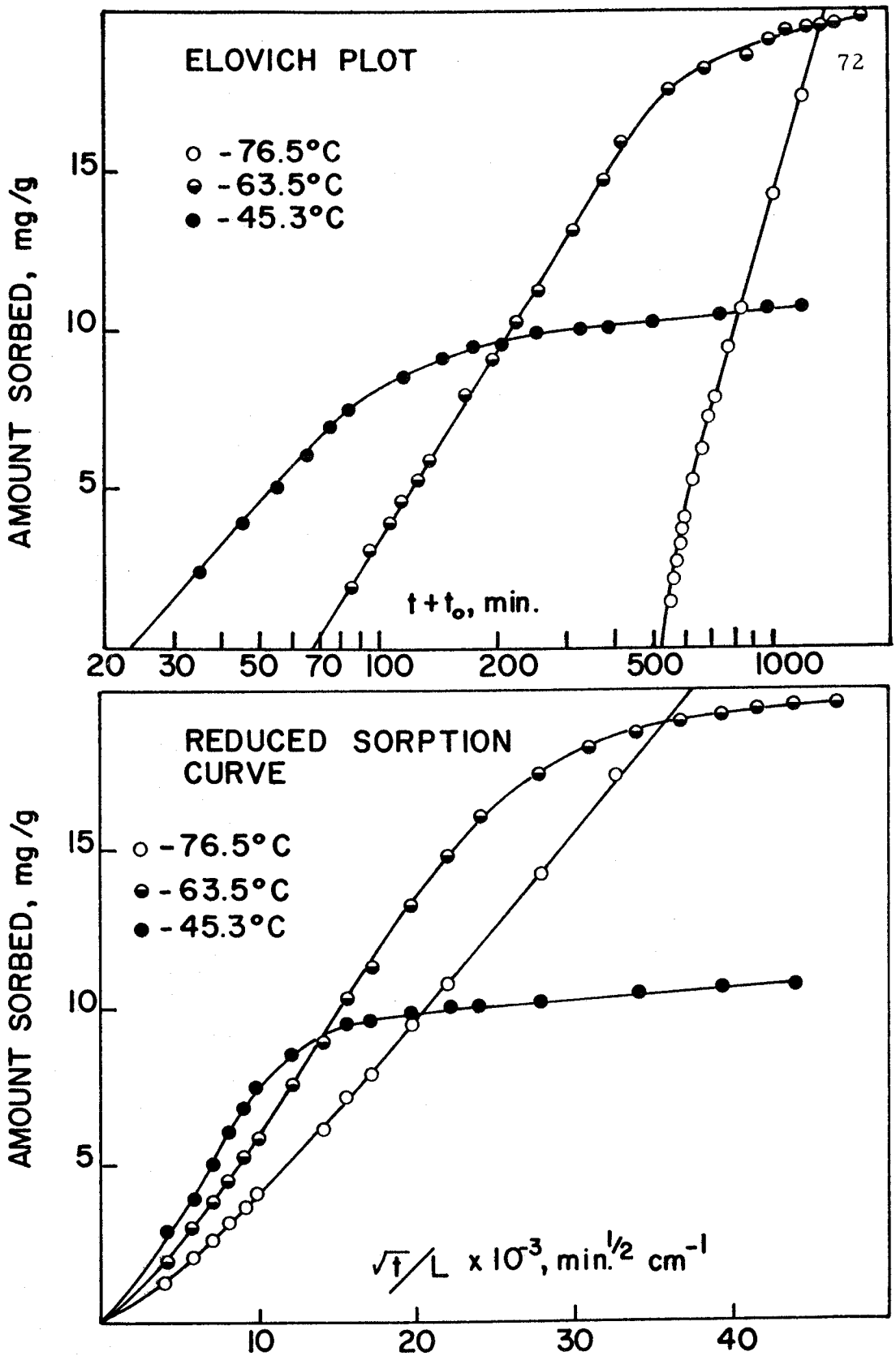


FIGURE 9. COMPARISON BETWEEN CHEMISORPTION THEORY AND DIFFUSION THEORY, SAMPLE I, 461 TORR.

no correlation was recognized that would aid in deciding which process was actually taking place. The isosteric heats listed in Table III are seen to rise with coverage and to roughly approach the heat of sublimation of $CO_2$. The rise of isosteric heats is interpreted as being caused by lateral interaction of the adsorbate molecules on a homogeneous surface. If the sorption process were chemisorption, a heterogeneous surface would be expected, some sites forming bonds with the adsorbate molecules more easily than others. This is what is normally observed in chemisorption, resulting in isosteric heats that decrease with temperature (32, p. 155-167). Also the values are very low for almost all chemisorption processes and the apparent approach to the heat of sublimation value for $CO_2$ strongly indicates a physical adsorption process. These isosteric heat values cannot be taken to be correct absolute values due to the problem of reversibility discussed previously. A strong hysteresis effect was found for water vapor sorption on these samples (28). Hence a strong possibility exists that there will also be hysteresis for $CO_2$ sorption. However, the trends shown by the isosteric heat values will still be valid and the actual numerical values should not be in serious error.

With the heat of adsorption values pointing toward physical rather than chemical adsorption and with the rate data lending itself to interpretation in terms of diffusion as well or better than in terms

of chemisorption, it was concluded that the process actually taking place is diffusion controlled physical adsorption. If complete adsorption isotherms could be obtained for $CO_2$ sorption on the eight organic films, this conclusion could probably be conclusively proven true or false. This was the case in the work of Slabaugh, et al. (26) on the sorption of water vapor on the same eight samples. However, at -76.5° C., where it is possible to achieve pressures (P) near a relative pressure ($P/P_o$) of one (where $P_o$ is the saturation pressure), the rate of $CO_2$ sorption is so slow as to make it experimentally almost impossible to measure a complete equilibrium isotherm. At higher temperatures, where the rate of interaction is fast enough to experimentally allow equilibrium to be reached, the saturation pressure of $CO_2$ is so high that relative pressure values over 0.2 to 0.3 cannot be reached. However, the conclusion reached regarding the type of interaction occurring is well substantiated in the literature. No cases of sorption of gases on polymer films interpreted in terms of chemisorption could be found. On the other hand, many cases were found where the interaction was interpreted as being a diffusion process, and several of these investigations will be cited in the next section.

## Diffusion and Diffusion Coefficients

The use of sorption techniques to measure diffusion coefficients of gases in polymers is a well established technique, especially for those systems which exhibit coefficients smaller than $10^{-9}$ cm.$^2$/sec. (19). Most of the sorption-diffusion studies have been done using water vapor as the adsorbate. Kumins, Rolle, and Roteman (13) studied the water vapor diffusion through a vinyl chloride-vinyl acetate copolymer. Hunt, et al. (11) investigated the sorption of water vapor by hydrophilic polymers and Spencer and Hunt (29) studied the kinetics of water vapor sorption by hydrophilic polymers.

An investigation by Kumins and Roteman (14), however, has permitted a direct comparison of diffusion coefficient values by carbon dioxide on the vinyl films. They studied the transport process of several gases differing in molecular diameter through a poly (vinyl chloride-vinyl acetate) copolymer. For carbon dioxide sorption they determined diffusion coefficients from $6.3 \times 10^{-8}$ cm.$^2$/sec. at 91° C. and 99 torr to $1.6 \times 10^{-10}$ cm.$^2$/sec. at 1° C. and 85 torr. The values obtained in this study are listed in Table VIII, samples 3 and 4 being the two vinyl films. If the downward trend of diffusion coefficients with temperature in the work of Kumins and Roteman is assumed to continue, it is seen that the diffusion coefficients for samples 3 and 4 would indeed be in the correct range. This agreement gives confidence to the values listed in Table VIII and lends support to the

belief that diffusion is actually the rate controlling mechanism.

It is seen from Table VIII that diffusion coefficients for all samples with the exception of 2 are within the same order of magnitude. The value for sample 2 was not obtained. In all cases, the values are concentration dependent, increasing with increasing carbon dioxide activity. Further, they are temperature sensitive, the rate of diffusion increasing with an activation energy on the order of 5 to 9 kcal/mole as is seen in Table IX.

If the heats of sorption given in Table III are compared to the activation energies of diffusion, it is seen that for samples 1 and 5, the activation energies are slightly greater. Thus it appears that for these two samples, the diffusing molecule has to acquire more energy than is necessary for the sublimation of $CO_2$ (assuming that the heats of sorption do indeed approximate the heat of sublimation of $CO_2$) to enable it to move from one equilibrium position to the next as it migrates into the sample. This additional energy is needed for the work which must be done in order to make a passage for the $CO_2$ molecule, a process usually referred to as "hole" formation (31). The activation energies for the other samples listed in the tables are approximately the same as the heat of sublimation of $CO_2$, or in the case of sample 8, slightly less. This can be interpreted on the basis that no energy is required for "hole" formation and for sample 8, that $CO_2$ is capable of diffusing without completely subliming. In

any case, the energies of "hole" formation required are relatively small, of the order of van der Waals forces or less, indicating that the size of the pores through which the gas diffuses is on the same order as the size of the $CO_2$ molecule.

A few values for the sorption and desorption coefficients for water vapor were determined for comparison purposes. The diffusion was found to be two to three orders of magnitude faster as can be seen from Table X. This faster rate of water vapor sorption has been attributed to the formation of hydrogen bonds in such a way that the "holes" in the polymer open up at a faster rate (14).

Valentine (33) studied the effect of crystallinity on the sorption of water vapor by polymers. He found that the crystalline portions of polymers were completely inaccessible to water vapor uptake. To check if crystallinity could be a factor in the sorption of $CO_2$, X-ray diffraction patterns were run on the polymer films. The results are listed in Table XI relative to a sample of polyethylene which showed one intense peak. Some mild crystalline character was exhibited by samples 1 and 5, and they are the samples sorbing the least amount of $CO_2$. However, this trend is not apparent with water vapor sorption (26). The other six samples showed no or very slight diffraction patterns. The difference of sorption for samples 1 and 5 is not large and without an extensive search into the problem, no conclusion can be drawn.

## Sorption of $CO_2$ and Filiform Corrosion

The investigation of $CO_2$ sorption on the organic films was initiated as part of a series of investigations of all atmospheric gases on these samples, since the atmosphere obviously has a part in the growth of filiform corrosion. The acidic nature of carbon dioxide suggests that it might act as a stimulant to the corrosion process in a manner similar to acetic acid. What is found is the exact opposite of this. Chan (4) in a series of exposure tests in controlled atmospheres found that $CO_2$ actually inhibited filiform growth. Maximum inhibition was found with a five percent $CO_2$ atmosphere. He postulated the formation of insoluble carbonates in the active filament head as being responsible for this inhibiting effect. Consequently, the rate at which $CO_2$ diffuses through the film into the active head region might be a factor in how well the film performs in preventing the corrosion.

Table I lists the relative filiform corrosion performance of the eight films investigated. These assignments were based on exposure studies (10) and are thus fairly qualitative in nature. However, if these values are examined in relation to the rates of $CO_2$ interaction, some correlation is seen to exist. Table XII lists the sample numbers in order of decreasing ability to prevent filiform corrosion. Also tabulated in order of decreasing values are the rates of $CO_2$ sorption as determined from the sorption coefficients, $\bar{R}_s$.

Table XII. Correlation of $CO_2$ diffusion rate and filiform corrosion resistance.

| Corrosion Performance (most resistant listed first) | Rate of $CO_2$ Sorption (most rapid listed first) |
|---|---|
| Sample 2 | Sample 8 |
| 8 | 1 |
| 1 | 5 |
| 7 | 7 |
| 6 | 4 |
| 5 | 3 |
| 4 | 6 |
| 3 | 2 |

Samples 8 and 1 exhibit the fastest rate of $CO_2$ sorption and are also the most resistant to corrosion. Samples 3 and 4 have relatively low rates of sorption and correspondingly low resistance to filiform corrosion. Samples 5 and 7 fall in the middle of each column. Samples 6 does not fit as clearly into this scheme. From its slow rate of sorption it should be fairly poor at resisting corrosion, but it appears to be moderately resistant to filiform corrosion. However, its overall uptake of $CO_2$ is relatively high and although the rate is slow the large amount sorbed may counteract the rate effect. Sample 2 appears to be a complete anomaly. It exhibits very high corrosion resistance and has the slowest sorption rate. Apparently some unique mechanism which has yet to be recognized is operating in the case of this phenolic film.

# BIBLIOGRAPHY


1. Asbeck, W. K., and M. Van Loo. Critical pigment volume relationship. Industrial and Engineering Chemistry 41: 1470-1475. 1949.

2. Barrer, R. M. Diffusion in and through solids. London, Cambridge University Press, 1941. 464 p.

3. Brunauer, Stephen, P. H. Emmett and Edward Teller. Adsorption of gases in multimolecular layers. Journal of the American Chemical Society 60:309-319. 1938.

4. Chan, Edmond James. The effect of oxygen, nitrogen, and carbon dioxide on filiform corrosion. Master's thesis. Corvallis, Oregon State University, 1963. 58 numb. leaves.

5. Crank, J. Mathematics of diffusion. London, Oxford University Press, 1956. 347 p.

6. Ehrlich, Sanford H. and Frederick A. Bettelheim. Infrared spectroscopy of the water vapor sorption process of mucopolysaccharides. Journal of Physical Chemistry 67:1954-1960. 1963.

7. Fujita, Hiroshi. Diffusion in polymer-diluent systems. Fortschritte der Hochpolymeren-Forschung. Advances in Polymer Science 3(1):1-47. 1961.

8. Glasstone, Samuel, Keith J. Laidler and Henry Eyring. The theory of rate processes. New York, McGraw-Hill, 1941. 611 p.

9. Hirst, W. The mechanical interaction between mobile insoluble adsorbed films, capillary condensed liquid and fine-structured solids. Discussions of the Faraday Society 3: 22-28. 1948.

10. Holboke, Lawrence Edwin. Adsorption isotherm studies of unsupported organic films. Master's thesis. Corvallis, Oregon State College, 1958. 44 numb. leaves.

11. Hunt, O. L., R. B. Huff and H. G. Spencer. Sorption of water vapor by hydrophilic polymers. Official Digest, Federation of Societies for Paint Technology 35:113-128. 1963.

12. Kaesche, H. Filiform corrosion of painted steel surfaces. Werkstoffe und Korrosion 11:668-681. 1959.

13. Kumins, C. A., C. J. Rolle and J. Roteman. Water vapor diffusion through vinyl chloride-vinyl acetate copolymer. Journal of Physical Chemistry 61:1290-1296. 1957.

14. Kumins, Charles A. and Jerome Roteman. Diffusion of gases and vapors through unpigmented vinyl films. Official Digest, Federation of Societies for Paint Technology 34:177-193. 1962.

15. Langmuir, Irving. Chemical reactions at low pressures. Journal of the American Chemical Society 37:1139-1167. 1915.

16. Long, F. A. and L. J. Thompson. Diffusion of water vapor in polymers. Journal of Polymer Science 25:413-426. 1955.

17. Low, M. J. D. Kinetics of chemisorption of gases on solids. Chemical Reviews 60:267-312. 1960.

18. McBain, J. W. and A. M. Bakr. A new sorption balance. Journal of the American Chemical Society 48:690-695. 1926.

19. Michaels, A. S., W. R. Vieth and H. J. Bixler. The measurement of diffusion coefficients of gases in polymers by sorption techniques. Journal of Polymer Science 1B: 19-23. 1963.

20. Patterson, Robert Joe. The interaction of nitrogen and carbon dioxide with unsupported organic films. Master's thesis. Corvallis, Oregon State University, 1961. 38 numb. leaves.

21. Pierce, Conway and R. Nelson Smith. Adsorption-desorption hysteresis in relation to capillary condensation. Journal of Physical Chemistry 54:784-794. 1950.

22. Prager, Stephen and F. A. Long. Diffusion of hydrocarbons in polyisobutylene. Journal of the American Chemical Society 73:4072-4075. 1951.

23. Preston, R. St. J. and B. Sanyal. Atmospheric corrosion by nuclei. Journal of Applied Chemistry 6:26-44. 1956.

24. Sarmousakis, J. N. and M. J. D. Low. Chemisorption data and the Elovich equation. Journal of Chemical Physics 25: 178-179. 1956.

25. Sharman, C. F. Filiform underfilm corrosion of lacquered steel surfaces. Nature 153:621-622. 1944.

26. Slabaugh, W. H. et al. Adsorption of water vapor by unsupported organic films. Journal of Applied Polymer Science 2:241-245. 1959.

27. Slabaugh, W. H. and Morris Grotheer. Mechanism of filiform corrosion. Industrial and Engineering Chemistry 46: 1014-1016. 1954.

28. Slabaugh, W. H. and G. Kennedy. Adsorption characteristics of organic films and filiform corrosion. Official Digest, Federation of Societies for Paint Technology 34:1139-1152. 1962.

29. Spencer, H. G. and O. L. Hunt. Kinetics of sorption of water vapor by hydrophilic polymers. Potassium and lithium forms of poly (vinyl methyl ether-maleic acid). Journal of Polymer Science 2A:5327-5335. 1964.

30. Taylor, H. A. and N. Thon. Kinetics of chemisorption. Journal of the American Chemical Society 74:4169-4173. 1952.

31. Thomas, A. Morris. Moisture permeability, diffusion and sorption in organic film-forming materials. Journal of Applied Chemistry 1:141-158. 1951.

32. Trapnell, B. M. W. Chemisorption. New York, Academic Press, 1955. 265 p.

33. Valentine, L. Studies of the sorption of moisture by polymers. I. Effect of crystallinity. Journal of Polymer Science 27: 313-333. 1958.

34. Van Loo, M., D. D. Laiderman and R. R. Bruhn. Filiform corrosion. Corrosion 9:277-285. 1953.

35. Young, D. M. and A. D. Crowell. Physical adsorption of gases. Washington, Butterworths, 1962. 426 p.